

Tuning Machine Learning Models for Prediction of Building Energy Loads

Saleh Seyedzadeh^{a,c,*}, Farzad Pour Rahimian^b, Parag Rastogi^c, Ivan Glesk^a

^a*Faculty of Engineering, University of Strathclyde, Glasgow, UK.*

^b*Faculty of Engineering & Environment, Northumbria University, Newcastle, UK.*

^c*arbnco, Glasgow, UK.*

Abstract

There have been numerous simulation tools utilised for calculating building energy loads for efficient design and retrofitting. However, these tools entail a great deal of computational cost and prior knowledge to work with. Machine Learning (ML) techniques can contribute to bridging this gap by taking advantage of existing historical data for forecasting new samples and lead to informed decisions. This study investigated the accuracy of most popular ML models in the prediction of buildings heating and cooling loads carrying out specific tuning for each ML model and using two simulated building energy data generated in EnergyPlus and Ecotect and compared the results. The study used a grid-search coupled with cross-validation method to examine the combinations of model parameters. Furthermore, sensitivity analysis techniques were used to evaluate the importance of input variables on the performance of ML models. The accuracy and time complexity of models in predicting heating and cooling loads are demonstrated. Comparing the accuracy of the tuned models with the original research works reveals the significant role of model optimisation. The outcomes of the sensitivity analysis are demonstrated as relative importance which resulted in the identification of unimportant variables and faster model fitting.

Keywords: Building energy loads, Energy prediction, Machine learning,

*Email: s.seyyedzadeh@gmail.com,
Address: 605, 75 Montrose St, Glasgow G1 1XJ

1 **1. Introduction**

2 Buildings must be designed to maximise the health and well-being of their
3 occupants while consuming the least energy and materials possible. Improving
4 the building stock to achieve this requires improvements to existing buildings in
5 addition to the construction of new high-performance buildings. One approach
6 to the design of high-performance buildings is performance-driven design, in
7 which the energy used by a building to keep its occupants comfortable is ap-
8 proximated using a physics-based simulation program. This method is called
9 Building performance Simulation (BPS), and it allows a designer/engineer to
10 examine the influence of form, materials, and systems before construction on
11 the expected thermal performance of a building. Conventionally, the search for
12 an optimal design with simulation has been through a manual iterative pro-
13 cess - design, analyse, change. This cycle is a labour-intensive task, so the
14 search space, i.e., the scope of possible options, is necessarily limited. The use
15 of performance-driven design can, thus, be augmented with optimisation, since
16 optimisation offers a way to significantly expand the search space during the
17 design process.

18 The benefits of optimisation over manual search are realised when the op-
19 timising routine is able to evaluate thousands of potential options (Si, 2017).
20 However, large runs of performance simulations of realistic building models re-
21 quire significant time and computational resources. Optimisation reduces the
22 specialist labour required to search very large spaces of options, but the result-
23 ing computational load can overwhelm the design process. The use of surrogate
24 models has been proposed to overcome this problem (Zhao & Magoulès, 2012a).
25 Surrogate or data-driven models are mathematical relationships between inputs
26 and outputs of interest from the system being studied, learnt from measured or
27 simulated data that represents the physical problem. For example, the thermo-
28 physical properties of building materials and weather parameters can be used

29 to predict indoor environmental conditions, as we do in this paper. Sufficiently
30 precise surrogate models, thus, provide fast and accurate alternatives to build-
31 ing performance simulators during a computationally-intensive design process
32 (Rastogi et al., 2017).

33 The use of surrogate models requires careful consideration of the accuracy
34 and appropriateness of the data and relationships inferred from the data. In
35 this paper, we examine a practical aspect of this approach: selecting and tuning
36 regression models for a given dataset. By this, we mean selecting the model
37 types, structures, and parameters most appropriate to the problem at hand.
38 As we have described in the next section, most previous work in using surro-
39 gate models in building simulation either compares linear models with nonlinear
40 models or different types of nonlinear models (Seyedzadeh et al., 2018). In ad-
41 dition, previous work has usually only optimised a limited number of model
42 parameters. The selection of model parameters, however, determines the per-
43 formance of a model on a given dataset, and this performance varies from one
44 dataset to another. Thus, the previous work does not provide a complete eval-
45 uation of different nonlinear models and does not provide sufficient guidance
46 about model selection. We show that the process of selecting a model must
47 account not just for predictive accuracy but also model complexity, ease of use,
48 and consistency of predictions. We use the datasets described by Rastogi et al.
49 (2017) and Tsanas & Xifara (2012) to demonstrate the performance of different
50 candidate models.

51 The paper is organised as follows. The next section presents a review of
52 previous studies and issues with using ML models in predicting building energy
53 consumption. That is followed by a description of the nonlinear methods evalu-
54 ated, the case studies, and results from our tuning proposals. The final section
55 contains recommendations on model selection and discusses future work.

56 **2. Background and Motivation**

57 This paper addresses the improvement of regression algorithms that relate
58 building characteristics with performance indicators of interest, e.g, insulation
59 level of walls with energy used for space heating. Broadly, regression approaches
60 are divided into two categories: supervised learning, in which the target is
61 known, and unsupervised learning, where there is no “output” to learn and pre-
62 dict. A supervised learning problem is either one of regression or classification.
63 In both cases, input features (X) are mapped to one or more output variables
64 (Y), such that changes in inputs cause the changes in output expected from the
65 real system being modelled. Unsupervised learning includes techniques such as
66 clustering, which organises data into groups based on similarities among the
67 samples in a dataset. Unsupervised learning is applied to an unlabelled dataset,
68 i.e., where there are no labels or target values for the model to learn from,
69 while a supervised learning algorithm can be tested against some ‘known’ labels
70 or values. In the use case demonstrated here, we have a database of inputs and
71 outputs obtained from a physics-based simulator, so this is a supervised learn-
72 ing exercise. This simulator is the ‘ground truth’, and the models are judged
73 solely on their ability to represent the simulator. We show how a model may
74 be improved to better represent the behaviour of a simulator while providing
75 estimates of outputs in a fraction of the time it would take the simulator to run
76 a simulation.

77 We will focus on nonlinear regression models, i.e., where the inputs cannot
78 be combined linearly, with or without any transformations. For example, a poly-
79 nomial model can be reformulated as a linear model of transformed (squared,
80 cubed, etc.) inputs but no such transformations can be applied to the inputs
81 of a Random Forest (RF) regression model. The use of machine learning (ML)
82 models in the analysis of buildings was first demonstrated by Kalogirou et al.
83 (1997) to estimate building heating loads considering envelope characteristic
84 and the desired (setpoint) temperature. Since then, the studies described below
85 have demonstrated that nonlinear models predict both simulated and metered

86 data better than linear models. Several studies have also presented compar-
87 isons between different nonlinear models. We now present an overview of the
88 literature, organised by the type of model(s) used in each study.

89 The pioneering work of Kalogirou et al. (1997) was completed in 2000 by
90 using Artificial Neural Networks (ANN) to predict the hourly energy demand of
91 holiday dwellings. Kalogirou et al. (2001) also used ANN to estimate the daily
92 heat loads of model house buildings with different combinations of the wall and
93 roof types (e.g., single vs cavity walls and roofs with different insulation) using
94 typical meteorological data for Cyprus. In that study, TRNSYS was used to
95 estimate energy use and the estimates were validated by comparing one building
96 with actual measurements. Similarly, Yokoyama et al. (2009) used a global
97 optimisation method coupled with the ANN to predict cooling load demand.
98 The authors probed two parameters of the network, namely the number of
99 hidden layers and the number of neurons in each layer.

100 Paudel et al. (2014) incorporated occupancy profiles as well as features rep-
101 resenting the operational heating power level and climate variables to model
102 the heating energy consumption. To increase the accuracy of the prediction
103 model, time-dependent attributes of operational heating power level were also
104 included. Deb et al. (2016) used five days' data as inputs to forecast the daily
105 cooling demand of three institutional buildings in Singapore. Mena et al. (2014)
106 applied ANN for short-term forecasting of hourly electricity consumption using
107 time series of solar production over two years in Spain. The resulting model
108 highlighted the significant impact of outdoor temperature and solar radiation
109 on electricity usage. Platon et al. (2015) used Principal Component Analysis
110 (PCA) to explore the selection of inputs for an ANN model in the prediction of
111 hourly electricity consumption of an institutional building. Li et al. (2015) also
112 used PCA to reduce the number of input variables, and introduced a new opti-
113 misation algorithm to improve the performance of an ANN model for short-term
114 forecasting of electricity demand. Neto & Fiorelli (2008) applied ANN to predict
115 the daily metered energy usage of a commercial building and demonstrated that
116 supervised learning could produce more accurate predictions than EnergyPlus

117 software. Improper assessment of lighting and occupancy was recognised as
118 the primary source of model uncertainty. Dombayci (2010) used degree-hours,
119 i.e., the difference between the external temperature and some nominal balance
120 point temperature integrated over time, to estimate the hourly energy demand
121 and used that as the output to be predicted. Due to its use of only degree-hours
122 the proposed approach was accurate only for the simplest residential buildings.

123 Yalcintas (2006) applied ANN to approximate the energy performance of
124 sixty educational buildings in Hawaii. The data was collected from energy
125 assessments reports and contained information about buildings and their air
126 conditioning systems. Wong et al. (2010) estimated the dynamic energy and
127 daylighting performance of a commercial building. The building daily energy
128 usage was calculated using EnergyPlus and coupled with an algorithm to ap-
129 proximate the interior reflections. Hong et al. (2014b) found that statistical
130 analysis was less accurate than ANNs in evaluating the energy performance
131 of schools in the UK. Khayatian et al. (2016) applied ANN to predict energy
132 performance certificates of domestic buildings in Italy. Ascione et al. (2017) in-
133 vestigated the association of energy usage and occupant thermal comfort in the
134 prediction of energy performance. The energy consumption was calculated using
135 EnergyPlus, and the ANN model trained on these was used as the calculation
136 engine to optimise building design and retrofit planning.

137 The use of Support Vector Machines (SVM) for forecasting building energy
138 consumption was introduced by Dong et al. (2005). The model was trained
139 with temperature, humidity, and solar radiation as the inputs. Li et al. (2009)
140 and Hou & Lian (2009) used SVM to forecast hourly cooling loads of an of-
141 fice building considering the same parameters suggested by Dong et al. (2005).
142 Massana et al. (2015) also investigated the short-term prediction of electricity
143 consumption using SVM. Xuemei et al. (2009) improved the performance of
144 SVM used for predicting cooling loads. Li et al. (2010) applied SVM for yearly
145 estimation of electricity consumption in domestic buildings. The model consid-
146 ered building envelope parameters as well as the annual electricity consumption
147 normalised by unit area. Zhao & Magoulès (2010) applied a parallel imple-

148 mentation of SVM to calculate energy usage for optimising the design of office
149 buildings. The work was improved by reducing the input variable space by ap-
150 plying gradient-guided feature selection and the correlation coefficients method.
151 Jain et al. (2014) investigated the impact of different time intervals and build-
152 ing spaces in data collection on energy demand forecasting using SVM. Finally,
153 Chen & Tan (2017) used an SVM model coupled with multi-resolution wavelet
154 decomposition for estimating energy consumption of various building type.

155 Since early 2000, Gaussian Process (GP) regression has been used by re-
156 searchers in different applications, especially where there are uncertainties in
157 input parameters (Grosicki et al., 2005; Bukkapatnam & Cheng, 2010). Heo
158 et al. (2012) and Heo & Zavala (2012) used GP modelling to estimate uncer-
159 tainty levels in calculating building energy saving after retrofitting. Zhang et al.
160 (2013) also applied GP to predict the post-retrofit energy demand of an office
161 building. Burkhart et al. (2014) incorporated GP with a Monte Carlo expect-
162 ation maximisation algorithm to train the model under data uncertainty, to
163 optimise the performance of the HVAC system of an office building. They found
164 that the models can be trained even with limited data or sparse measurements
165 when precise and extensive sensor data is not available. Rastogi et al. (2017)
166 compared the accuracy of GP and linear regression in emulating of a building
167 performance simulation and show that the accuracy of GP is four times better
168 than linear regression.

169 Though ensemble ML models such as Random Forest (RF) and Gradient
170 Boosted Regression Trees (GBRT) have been around for decades, their use in
171 estimating building energy consumption is very new. Tsanas & Xifara (2012)
172 applied RF to estimate energy consumption using building characteristics and
173 showed that it performed better than the iteratively re-weighted least squares
174 method. Papadopoulos et al. (2017) compared tree-based models in building
175 energy performance estimation using the data provided by Tsanas & Xifara
176 (2012). Recently, Wang et al. (2018) used RF for short-term prediction of
177 energy usage in an office building considering compound variables of envelope,
178 climate, and time.

179 Yalcintas & Ozturk (2007) and Yalcintas (2006) compared the accuracy
180 of Artificial Neural Networks (ANN) with that of Multiple Linear Regression
181 (MLR) to estimate the energy performance of commercial buildings, while Hong
182 et al. (2014a) compared ANN with physics-based models for the same use case.
183 Platon et al. (2015) compared ANN with case-based reasoning (CBR) for pre-
184 diction of hourly electricity consumption of an institutional building. Li et al.
185 (2009) applied SVM to forecast hourly cooling loads of an office building and
186 provided a comparison with ANN, indicating that the ANN had more potential.
187 However, Edwards et al. (2012) also evaluated the accuracy of SVM and ANN in
188 forecasting hourly energy consumption of residential buildings and found ANN
189 to be the least accurate model. Zhang et al. (2015) compared change-point
190 models with Gaussian-based and one layer ANN models to predict the energy
191 consumed by an office building to supply hot water and concluded that ANN
192 models can be inefficient when enough data is not available. Tsanas & Xifara
193 (2012) investigated the accuracy of RF and iteratively re-weighted least squares
194 regression model. Wang et al. (2018) indicated the superiority of RF over SVM
195 and regression trees in predicting hourly building energy demands.

196 *2.1. Gaps*

197 As the survey of literature in this section shows, there is a wealth of examples
198 of nonlinear regression models (machine learning) applied to problems related to
199 predicting energy and mass flows in buildings. Each study demonstrates the use
200 of one model type/architecture or comparison between different model types.
201 However, there is a lack of guidance on how to optimise or ‘tune’ models to fit the
202 problem at hand for the best predictive accuracy and consistency. This paper,
203 therefore, lays out a widely-applicable approach to tuning nonlinear models to
204 building energy data. Though the examples shown here are from simulators,
205 the method is also applicable to measured data.

206 **3. Machine Learning Models**

207 ML models operate as a black box, so further information about the building
208 is not required. The general scheme of supervised learning for modelling building
209 energy is illustrated in Figure 1. As seen, the first step is to select a set of
210 features for representing the building energy system. Although data-driven
211 methods build models with fewer variables than engineering techniques, it is
212 crucial to generate a logical input set for the ML model. These features are not
213 necessarily raw building characteristics or weather data; instead, they could be
214 complex variables calculated from basic ones, e.g. wall to floor ratio and mean
215 daily global radiation (Zhao & Magoulès, 2012b).

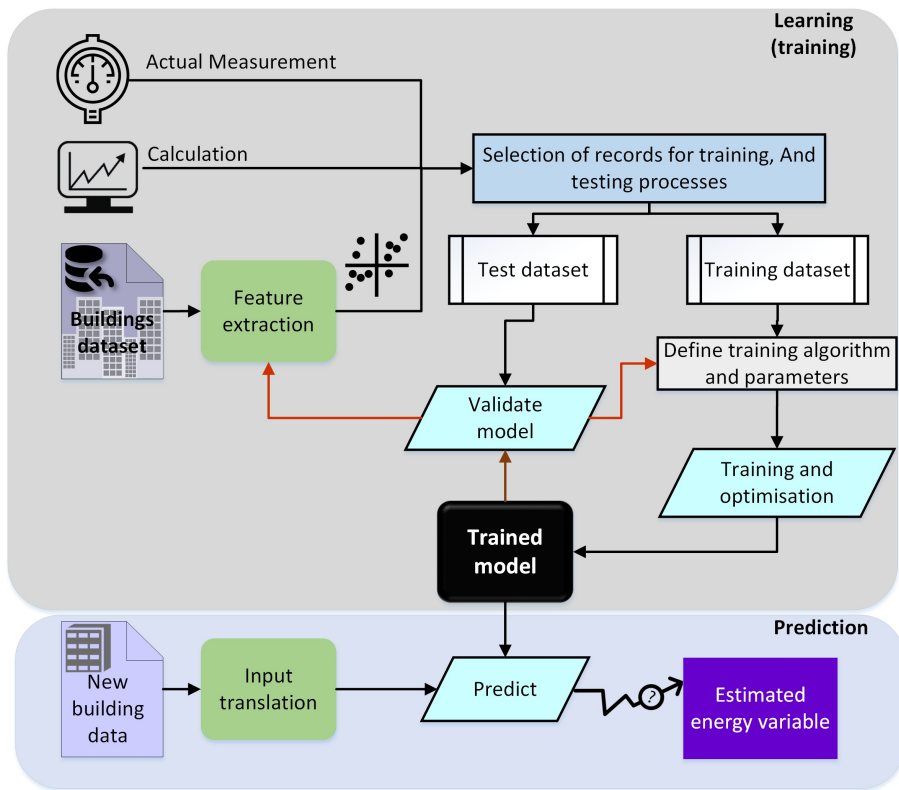


Figure 1: General schematic diagram of supervised learning.

216 The next key stage in utilising MLs is optimisation of model itself. This

217 procedure which is called tuning plays an important role in the performance
218 of an ML model especially when it is a complex one. Choosing inappropriate
219 hyper-parameters will result in poor accuracy which may falsely be translated
220 as the model failure. Although selecting the right input variables is essential
221 for training a successful machine, the full advantage cannot be taken of ML
222 without tuning the model for that specific training data. Each ML has different
223 hyper-parameters which govern the learning process. A key point in tuning
224 an ML model parameters is the generalisation. That is to say, how well the
225 learning model applies to specific examples not seen by the model when it was
226 training. Hence, in the procedure of model optimisation, there should be a
227 proper mechanism such as cross-validation to avoid overfitting (i.e. modelling
228 the training data too well).

229 Five ML techniques including ANN, SVM, GP, RF and GBRT are employed
230 to emulate two BPS tools namely EnergyPlus and Ecotect. A standard method
231 that we used to select optimal hyper-parameters is a grid-search combined with
232 k-fold cross-validation. In this procedure, the data is divided into k exclusive
233 subsets, and each combination of model parameters and architecture is fitted to
234 each distinct group of $k - 1$ subsets and tested on the remaining subset. This
235 process provides a distribution of errors for a given model choice on different
236 parts of the dataset, i.e., an estimate of the general applicability of the model
237 to represent the variation in the dataset. Furthermore, different normalisations
238 such as standard, min-max and robust are applied to data before training pro-
239 cedure. Robust scaler eliminates the median and normalises data according to
240 the inter-quartile range.

241 Basics of each model and the parameters going under optimisation are ex-
242 plained as followings.

243 *3.1. Artificial Neural Network*

244 Neural networks have been broadly utilised for building energy estimation
245 and known as the major ML techniques in this area. They have been successfully
246 used for modelling non-linear problems and complex systems. By applying

247 different techniques, ANNs have the capability to be immune to the fault and
248 noise (Tso & Yau, 2007) while learning key patterns of building systems.

249 The main idea of ANN is obtained from the neurobiological field. Several
250 kinds of ANN have been proposed for different applications including, Feed
251 Forward Network (FFN), Radial Basis Function Network (RBFN) and recurrent
252 networks (RNN). Each ANN consists of multi-layers (minimum two layers) of
253 neurons and activation functions that form the connections between neurons.
254 Some frequently used functions are linear, sigmoid and hard limit functions (Park
255 & Lek, 2016).

256 In FFN which was the first NN model as well as the simplest one, there are
257 no cycles from input to output neurons and the pieces of information moves in
258 one direction in the network. Figure 2 illustrates the general structure of FFN
259 with input, output and one hidden layer.

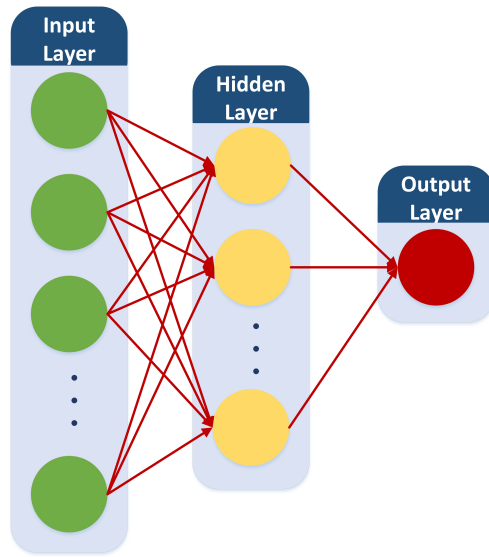


Figure 2: Conceptual structure of feed forward neural network with three layers.

260 RNN uses its internal memory to learn from preceding experiences by allow-
261 ing loops from output to input nodes. RNN is proposed in various architectures
262 including fully connected, recursive, long short-term memory, etc. This type

263 of neural network has usually been employed to solve very deep learning tasks
264 such as multivariate time-series prognostication; often more than 1000 layers
265 are needed (Ghiassi et al., 2005).

266 In RBFM, a radial basic function is used as activation function providing
267 a linear combination of inputs and neuron parameters as output. This type of
268 network is very effective for time series estimation (Harpham & Dawson, 2006;
269 Leung et al., 2001; Park et al., 1998).

270 Due to the nature of the datasets, a multilayer perception FFN is utilised in
271 this work. The ANN hyper-parameters which go under optimisation are:

- 272 • **Optimiser:** the function that updates the weights and bias;
- 273 • **Activation:** a non-linear transformation function which is applied over
274 the input, and then the output is fed to the subsequent layer neurons as
275 input. An ANN without activation function will act as a linear regressor
276 and may fail to model complex systems;
- 277 • **Initialisation:** the initial values of weights before the optimiser is applied
278 for training;
- 279 • **Epoch:** the number of forward and backward passes for all samples of
280 data;
- 281 • **Batch size:** specifies the number of samples that are propagated through
282 the ANN training (i.e. the number of samples in one epoch);
- 283 • **Dropout rate:** dropout is a regularisation method for preventing ANN
284 from overfitting and creating more generalised model by randomly reject-
285 ing some neurons during training. Dropout rate determines the percentage
286 of randomly input exclusion at each layer;
- 287 • **Size:** number of neurons in each layer and number of layers.

288 3.2. Support Vector Machine

289 SVMs are highly robust models for solving non-linear problems and used in
290 research and industry for regression and classification purposes. As SVMs can

291 be trained with few numbers of data samples, they could be right solutions for
 292 modelling study cases with no recorded historical data. Furthermore, SVMs
 293 are based on the Structural Risk Minimisation (SRM) principle that seeks to
 294 minimise an upper bound of generalisation error consisting of the sum of train-
 295 ing error and a confidence level. SVMs with kernel function acts as a two-layer
 296 ANN, but the number of hyper-parameters is fewer than that. Another advan-
 297 tage of SVM over other ML models is uniqueness and globally optimality of
 298 the generated solution, as it does not require non-linear optimisation with the
 299 risk of sucking in a local minimum limit. One main drawback of SVM is the
 300 computation time, which has the order almost equal to the cube of problem
 301 samples.

302 Suppose every input parameter comprises a vector X_i (i denotes the i th
 303 input component sample), and a corresponding output vector Y_i that can be
 304 building heating loads, rating or energy consumption. SVM relates inputs to
 305 output parameters using the following equation:

$$Y = W \cdot \phi(X) + b \quad (1)$$

306 where $\phi(X)$ function non-linearly maps X to a higher dimensional feature
 307 space. The bias, b , is dependent of selected kernel function (e.g. b can be
 308 equal to zero for Gaussian RBF). W is the weight vector and approximated by
 309 empirical risk function as:

$$\text{Minimise} : \frac{1}{2} \|W\|^2 + C \frac{1}{1} \sum_{i=1}^N L_{\varepsilon}(Y_i, f(X_i)) \quad (2)$$

310 L_{ε} is ε -intensity loss function and defined as

$$L_{\varepsilon}(Y_i, f(X_i)) = \begin{cases} |f(x) - Y_i| - \varepsilon, & |f(x) - Y_i| \geq \varepsilon \\ 0, & \text{otherwise} \end{cases} \quad (3)$$

311 Here ε denotes the domain of ε -insensitivity and N is the number of training
 312 samples. The loss becomes zero when the predicted value drops within the band
 313 area and gets the difference value between the predicted and radius ε of the

314 domain, in case the expected point falls out of that region. The regularised
 315 constant C presents the error penalty, which is defined by the user.

316 SVM rejects the training samples with errors less than the predetermined ε .
 317 By acquisition slack variables ξ and ξ_i^* for calculation of the distance from the
 318 band are, equation (3) can be expressed as:

$$\underset{\xi, \xi_i^*, W, b}{\text{Minimise}} : \frac{1}{2} \|W\|^2 + C \frac{1}{N} \sum_{i=1}^N \xi + \xi_i^* \quad (4)$$

319 subject to

$$\begin{cases} Y_i - W \cdot \phi(x_i) - b \leq \varepsilon + \xi \\ W \cdot \phi(x_i) + b - Y_i \leq \varepsilon + \xi_i^* \\ \xi \geq 0, \quad \xi_i^* \geq 0 \end{cases} \quad (5)$$

320 The SVM problem using a kernel function of $K(X_i, X_j)$ (α_i, α_i^* as Lagrange
 321 multipliers) can be simplified as:

$$\underset{\{\alpha_i\}, \{\alpha_i^*\}}{\text{Maximise}} : -\varepsilon \sum_{i=1}^N (\alpha_i^* + \alpha_i) + \sum_{i=1}^N Y_i (\alpha_i^* - \alpha_i) - \frac{1}{2} \sum_{i=1}^N \sum_{j=1}^N (\alpha_i^* - \alpha_i) (\alpha_j^* - \alpha_j) K(X_i, X_j) \quad (6)$$

322 subject to

$$\sum_{i=1}^N (\alpha_i^* - \alpha_i) = 0, \quad 0 \leq \alpha_i, \alpha_i^* \leq C \quad (7)$$

323 As mentioned before the number of parameters in SVM with a Gaussian
 324 RBF kernel is few as two which are C and Gamma.

325 3.3. Gaussian Process

326 The main drawback of GP modelling is expensive computational cost, es-
 327 pecially with the increase of training samples. This is due to the fact that GP

328 constructs a model by determining the structure of a covariance matrix com-
 329 posed of $N \times N$ input variable where the matrix inversion required in predictions
 330 has a complexity of $O(N^3)$

331 Given a set of n independent input vector X_j ($j = 1, \dots, n$), the correspond-
 332 ing observations of y_i ($i = 1, \dots, n$) are correlated using covariance function K
 333 with normal distribution equal to (Li et al., 2014):

$$P(y; m; k) = \frac{1}{(2\pi)^{n/2} |K(X, X)|^{1/2}} \times \exp\left(-\frac{1}{2}(y - m)^T K(X, X)^{-1}(y - m)\right) \quad (8)$$

334 The covariance or kernel function can be derived as

$$K = \begin{vmatrix} k(x_1, x_1) & k(x_1, x_2) & \cdots & k(x_1, x_n) \\ k(x_2, x_1) & k(x_2, x_2) & \cdots & k(x_2, x_n) \\ \vdots & \vdots & \ddots & \vdots \\ k(x_n, x_1) & k(x_n, x_2) & \cdots & k(x_n, x_n) \end{vmatrix} \quad (9)$$

335 A white noise, σ , is presumed in order to consider the uncertainty. It is
 336 assumed that the samples are corrupted (lets suppose as new inputs as x^*) by
 337 this noise. In this case covariance of y is expressed as

$$\text{cov}(y) = K(X, X) + \sigma^2 \quad (10)$$

338 Then y^* can be estimated as below.

$$y^* = \sum_{i=1}^n \alpha_i k(x_i, x^*) \quad (11)$$

$$\alpha_i = (K(X, X) + \sigma^2 I)^{-1} y_i \quad (12)$$

339 For GP model three parameters are tuned: kernel, alpha (α) which is the
 340 value added to the diagonal of the kernel matrix (equation 11) and the number
 341 of restarts of the optimiser for discovering the parameters maximising the log-

342 marginal probability. Two combinations of white noise with RBF and Matern
343 covariance functions are used for GP model kernel. Matern kernel is denied as:

$$K(X, X') = \frac{261 - v}{\Gamma(v)} \left(\frac{\sqrt{2v} |x - x'|}{I} \right)^v K_v \left(\frac{\sqrt{2v} |x - x'|}{I} \right) \quad (13)$$

344 Here, Γ is the Gamma function and K_v is the modified Bessel function the
345 second-order v (Owen et al., 1965).

346 3.4. *Random Forest*

347 Random forest is a collection (ensemble) of randomised decision trees (DTs)
348 (Tin Kam Ho, 1995). DT is a non-parametric ML that establishes a model
349 in the form of a tree structure. DT repeatedly divides the given records into
350 smaller and smaller subsets until only one record remains in the subset. The
351 inner and final sets are known as nodes and leaf nodes. As the precision of DT
352 is substantially subject to the distribution of records on in the learning dataset,
353 it is considered as an unstable method (i.e. tiny alteration in the observations
354 will change the entire structure). To overcome this issue a set of DTs and
355 uses the average predicted values of all independent trees as the final target. In
356 general, RF applies bagging to combine separate models but with sore of similar
357 information and generate a linear combination from many independent trees.

358 RF requires few number of hyper-parameters to be set. The main parameter
359 is the number of independent trees in the forest. There is a trade-off between
360 the accuracy of model and training/prediction computational cost. Thereby,
361 this parameter should be tuned to choose the optimal value. Other parame-
362 ters include the number of features to consider when seeking for the best split,
363 whether bootstrap samples are used when creating trees and minimum number
364 of data sample to split a node and required in each node.

365 3.5. *Gradient Boosted Regression Trees*

366 Like RF, GBRT is an ensemble of other prediction models such as DTs. The
367 principal difference between GBRT and RF is that the latter one is based on fully
368 developed DTs with low bias and high variance, while the former employs weak

369 learners (small trees) having high bias and low variance (Breiman, 2017). In
370 GBRT, trees are not independent of each other; instead, each branch is created
371 based on former simple models through a weighting procedure. This approach
372 is known as boosting algorithm. At each inner node (i.e. the split point) given
373 dataset is divided into two samples. Let's assume a GBRT with three nodes
374 trees; then there will be one split point in which the best segmentation of the
375 data is decided, and the divergence of the obtained values (from the individual
376 averages) are calculated. By fitting on these residuals, the subsequent DT will
377 seek for another division of data to reduce the error variance.

378 Most important parameters for optimising GBRT comprise learning rate
379 (also known as shrinkage) which is a weighting procedure to prevent overfitting
380 by controlling the contribution of each tree, number of trees, maximum depth
381 of tree and the number of features for searching best division, and the minimum
382 number of data sample to split a node and required in each node. Moreover,
383 the sub-sample parameter defines the fraction of observation to be selected for
384 each tree.

385 Rather than conventional GBRT model the recently improved version known
386 as eXtreme Gradient Boosting (XGBoost) algorithm (Chen & Guestrin, 2016)
387 is also evaluated with similar parameters, but some differences. The minimum
388 sum of instance weight controls the generalisation similar to minimum sample
389 split in GBRT. The portion of columns when constructing each tree (colsample
390 bytree) similar to maximum features.

391 *3.6. Performance Evaluation*

392 Various measurements based on actual and predicted results are calculated,
393 in order to evaluate the performance or accuracy of data-driven models. These
394 include Coefficient of Variance (CV), Mean Bias Error (MBE), Mean Squared
395 Error (MSE), Root Mean Squared Error (RMSE), Mean Squared Percentage
396 error (MSPE), Mean Absolute Percentage Error (MAPE) and MAE (mean ab-
397 solute error). CV is the variation of overall prediction error concerning actual
398 mean values. MBE is used to determine the amount over/underestimation of

399 predictions. MSE and MSPE is a good inductor of estimation quality. MAE
400 determines the average value of the errors in a set of forecasts and MAPE is the
401 percentage of error per prediction. RMSE has the same unit of actual measure-
402 ments. In this work, RMSE, MAE and **coefficient of determination** (R^2)
403 are used to present the accuracy of ML models. R^2 is the percentage variance
404 in the dependent variable explained by the independent ones. These values are
405 calculated as follows:

$$RMSE = \sqrt{\frac{1}{N} \sum (y_i - \hat{y})^2} \quad (14)$$

$$MAE = \frac{1}{N} \sum |y_i - \hat{y}| \quad (15)$$

$$R^2 = \frac{\sum (\hat{y}_i - \bar{y})^2}{\sum (y_i - \bar{y})^2} \quad (16)$$

406 Here, y , \hat{y} and \bar{y} represent the real, estimated and average response values,
407 respectively.

408 4. Selected Datasets for Case Study

409 Two building datasets simulated using BPS tools are utilised. First data
410 contains 768 variations of a residential building obtained altering eight basic
411 envelope characteristic (Tsanas & Xifara, 2012), and the second dataset includes
412 various building type represented by 28 envelope and climate features (Rastogi,
413 2016). Each set and the distribution of variables are presented in this section.
414 The prediction targets for both sets are heating and cooling loads.

415 4.1. Ecotect Dataset

416 This dataset was developed by Tsanas & Xifara (2012) and obtained from
417 UCI machine learning repository (Xifara & Tsanas, 2012). It includes 12 resi-
418 dential buildings types with the same volume ($771.75m^3$) and varying envelope
419 features, outlined in Table 1. The materials were chosen to achieve the lowest

420 U-values based on availability in the market (walls: $1.78 \text{ m}^2\text{K}/\text{W}$, floors: 0.86,
421 roofs: 0.50 and windows: 2.26). The window-to-floor ratio is varied from 0%
422 to 40%. The glazing distribution on each faade has 6 variants: (0) uniform,
423 with 25% glazing on each side; (1) 55% glazing on the north faade and 15%
424 on the rest; (2) 55% glazing on the east faade and 15% on the rest; (3) 55%
425 glazing on the south faade and 15% on the rest; (4) 55% glazing on the west
426 faade and 15% on the rest; and, (5) no glazing. All combinations were simu-
427 lated using Ecotect with weather data from Athens, Greece, and occupancy by
428 seven people conducting mostly sedentary activities. The ventilation was run in
429 a mixed mode with 95% efficiency and thermostat setpoint range of $19\text{-}24^\circ\text{C}$.
430 The operating hours were set to 3 pm - 8 pm (15:00-20:00) for weekdays and
431 10 am - 3 pm (10:00-15:00) for weekends. The lighting level was set to 300 lx.
432 Figure 3 illustrates the frequency distribution of features and the correlation
433 between each pair of input and target variables is plotted as a heat map matrix
434 in Figure 4.

435 Figure 3 illustrates the frequency of features as histogram graphs. The
436 correlation between each pair of input and target variables is demonstrated
437 using heatmap matrix in Figure 4.

438 4.2. *EnergyPlus Dataset*

439 This datasets consists of commercial and residential buildings and is de-
440 scribed by Rastogi (2016). The original commercial building models were down-
441 loaded from the US Department of Energy (USDOE) commercial reference
442 building models (DOE). The commercial buildings set includes sixteen types
443 of buildings classified into eight overall groups based on usage. Table 2 presents
444 the building types which are considered in the simulations and the frequency
445 of each with unique features. For each subtype, there are three variations for
446 envelope construction: pre-1980, post-1980, and new construction. Each usage
447 type has the same form, area and operation schedules. The residential build-
448 ings are described by Chinazzo et al. (2015). Variation in the outputs is also
449 introduced by considering several years of historical weather data from many

Table 1: List of features that represent the characteristics of residential buildings for prediction of energy loads

Feature	Unit	Range	Variation	Code
Inputs				
Relative compactness	-	0.62 – 0.98	12	rc
Surface area	m^2	514 – 808	12	sa
Wall area	m^2	245 – 416	7	wa
Roof area	m^2	110 – 220	4	ra
Overall height	m	3.5, 7	2	oh
Orientation	-	2 – 5	4	ori
Glazing area	m^2	0 – 0.4	4	glza
Glazing area distribution		0 – 5	6	glzd
Targets				
Heating load	KWh/m^2	6 – 43	-	heat
Cooling load	KWh/m^2	10 – 48	-	cool

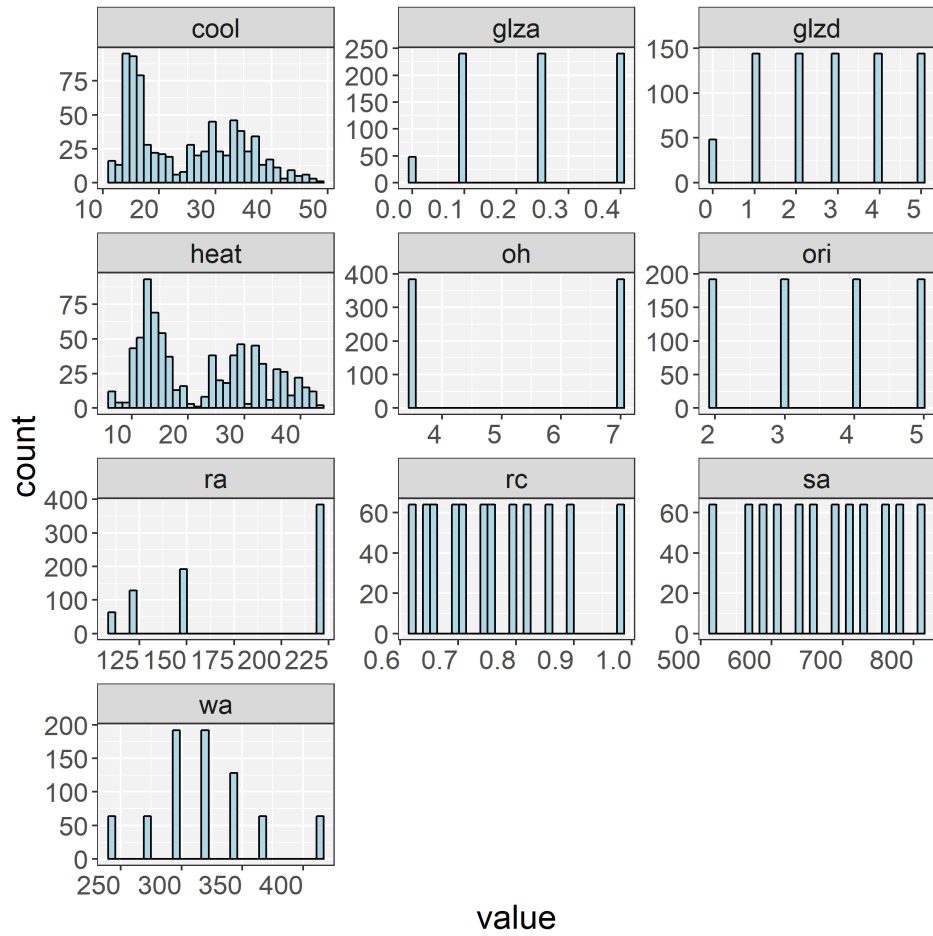


Figure 3: Distribution of features for Ecotect data.

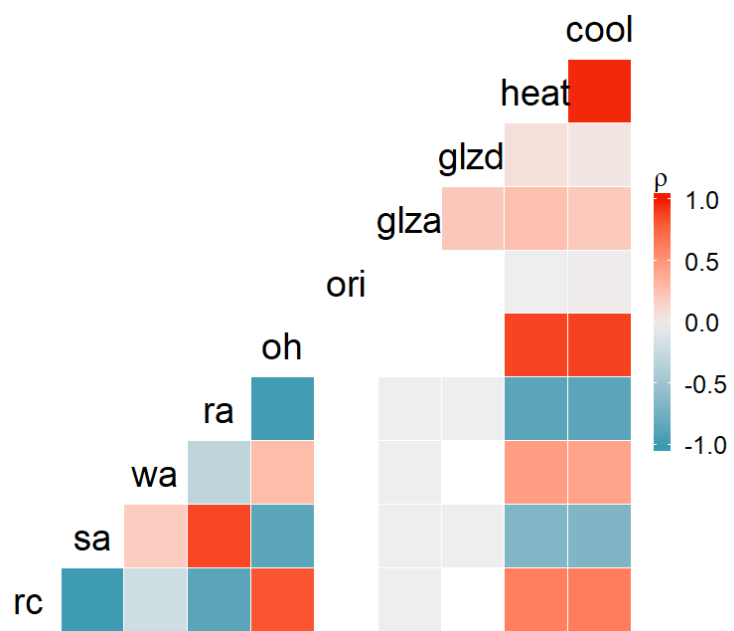


Figure 4: Ecotect data features correlation map.

450 climates (weather stations) and augmenting this data with synthetic weather
451 generated for some climates (Rastogi, 2016).

452 We use the same regression inputs as originally proposed in (Rastogi & An-
453 dersen, 2016). They describe the feature selection as being based on correlation
454 estimation and Principal Component Analysis (PCA). There are three kinds
455 of input variables: climate, building, or mixed. The climate variables were ex-
456 tracted from one year of weather data only and are independent of the buildings
457 simulated. The building features are related to the physical characteristics of
458 the building envelope and independent of the climate. These inputs were cho-
459 sen on the basis of impact on the heating and cooling loads and calculated from
460 geometry, material and structure properties. The mixed parameters represent
461 the interactions between weather and buildings. An input that does not belong
462 to any of these categories, the internal heat gain, was also included to represent
463 the impact of human behaviour. Figure 5 and Figure 6 illustrate the frequency
464 of features and correlation heat-map matrix respectively.

465 Figure 5 illustrates the frequency of features as histogram graphs for Ener-
466 gyPlus Dataset. It can be seen that the each variable is relatively distributed
467 over the possible predefined values. The correlation heat-map matrix presented
468 in Figure 6 shows the in dependency of different features especially building
469 physics related ones from each other.

470 **5. Result and Discussions**

471 All models are implemented using Python programming language and test
472 have been carried out on a PC with Intel Core i7-6700 3.4GHz CPU, 32GB
473 RAM.

474 The stated goal of this paper is to highlight the importance of tuning nonlin-
475 ear regression models (ML models) to achieve the best predictive performance
476 for a given use case. To put our work in context, it is worth noting the results
477 from the original studies that introduced the datasets used in this paper (Tsanas
478 & Xifara, 2012; Rastogi et al., 2017). Tsanas & Xifara (2012) reported RMSEs of

Table 2: Frequency and size of building types in EnergyPlus data

Building Usage	Type	Area (m^2)	Volume (m^3)	No. of E+ zones	No. of samples
Health	Hospital	22,422	88,864	55	3827
	Outpatient	3,804	11,932	118	5504
Home	Mid-rise	3,135	9,553	36	37173
	Apartment				
	Single Family	78532			
Hotel	Large	11,345	35,185	43	5504
	Small	4,014	11,622	67	5468
Office	Large	46,320	178,146	73	275345
	Medium	5503	4,982	18	19,741
	Small	511	1,559	5	5483
Restaurant	Full Service	5,502	55,035	2	3824
	Quick Service	232	708	2	5505
Retail	Stand Alone	2,294	13,993	5	5503
	Strip_Mall	2,090	10,831	10	5498
	Supermarket	45,002	900,272	6	5554
School	Primary	6,871	27,484	25	5505
	Secondary	19,592	95,216	46	5507
Warehouse	–	4,835	39,241	3	5492

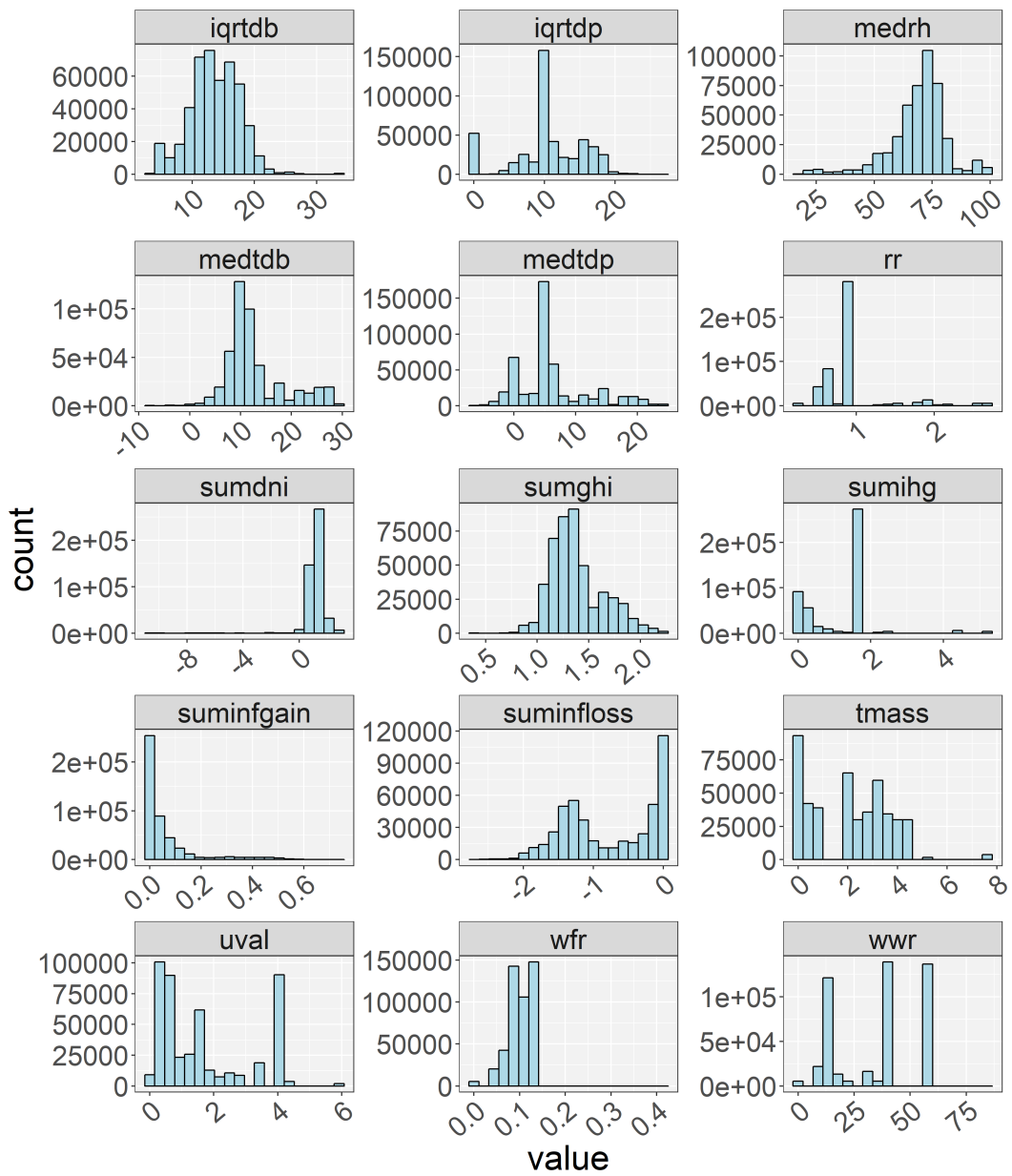


Figure 5: Distribution of features for EnergyPlus data.

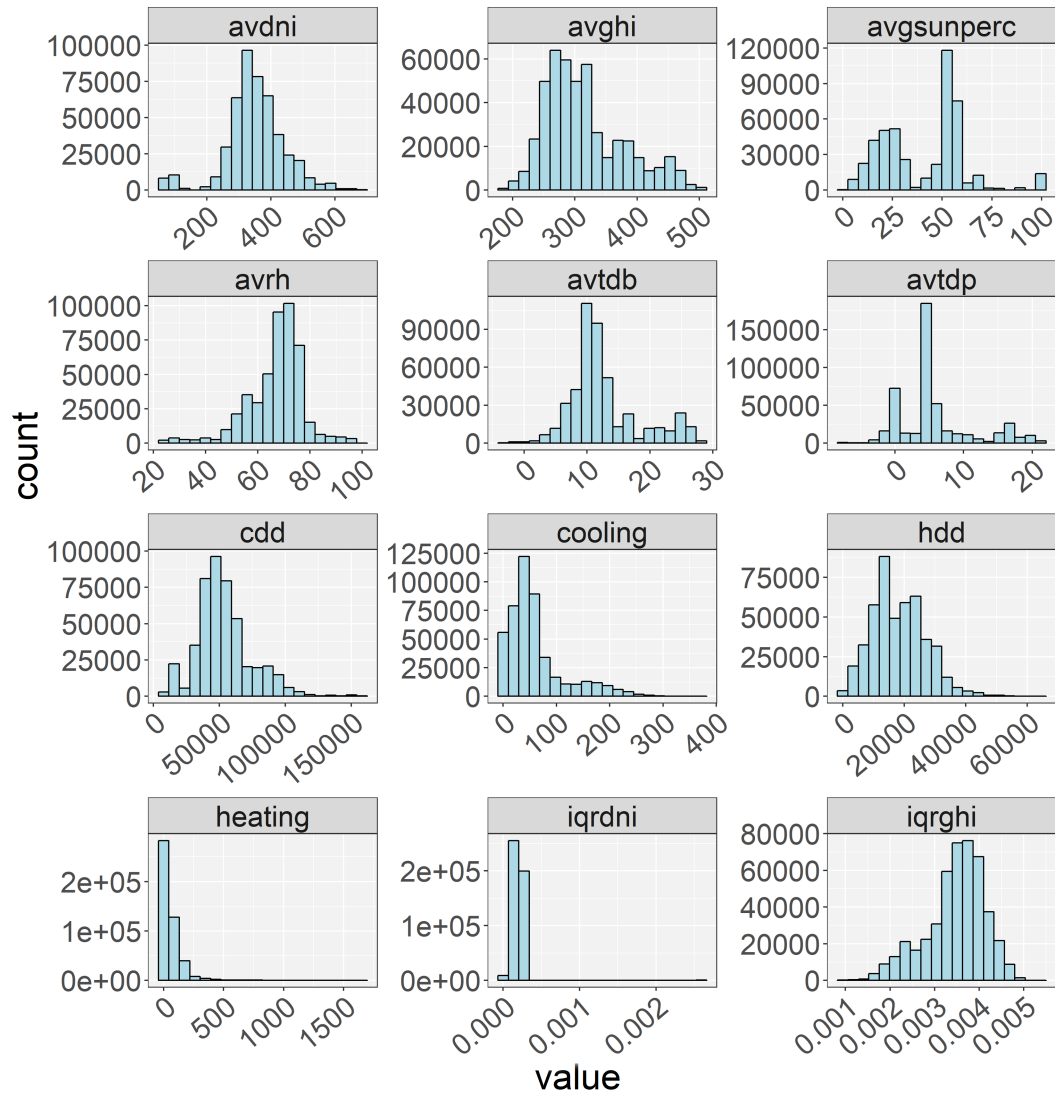


Figure 5 (Cont.): Distribution of features for EnergyPlus data.

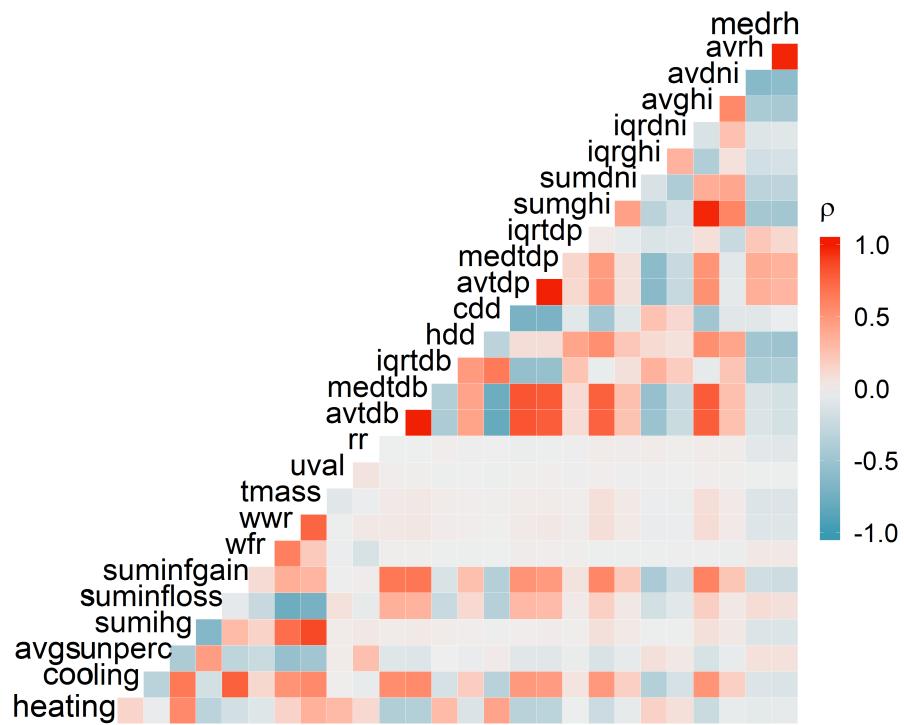


Figure 6: EnergyPlus data features correlation map.

Table 3: List of EnrgyPlus features extracted for model training

Group	QTY	Stats	Description	Range	Code	Unit
Building	U-value	Average	Average U-value of envelope	0.14–6.06	<i>uval</i>	W/m^2K
	Thermal Mass	Sum	Sum of thermal storage capacity	1e-4–7.61	<i>tmass</i>	MWh/K
	Envelope Ratios	Ratio	Ratio of window area to wall area	0.58–85.00	<i>wwr</i>	-
			Ratio of window area to floor area	0.01–0.42	<i>wfr</i>	-
	Massing	Ratio	Form Factor (Volume / Wall Area)	2.47–17.14	<i>ff</i>	-
			Roof Ratio (Roof / Wall Area)	0.31–2.73	<i>rr</i>	-
Mixed	Shading	Average	Average sunlit percentage of envelope	0.35–100	<i>avgsunperc</i>	%
	Infiltration	Sum	Annual sum of energy gained due to infiltration	0–0.74	<i>suminfgain</i>	GWh
			Annual sum of energy lost due to infiltration	-2.7–-1e-4	<i>suminfloss</i>	
Other	Sum	Annual sum of Internal Heat Gain	0.03–5.24	<i>sumIHG</i>	GWh	

479 1.014 and 2.567 for heating and cooling loads, respectively. Our best RF model
480 achieved 0.476 and 1.585 for the same variants, a roughly 40% improvement in

List of features extracted for model training (cont.)

GRP	QTY	Stats	Name	Range	Code	Unit
Climate	Degree Days	Sum	Annual sum of cooling degree days	(9.6–160)e4	<i>cdd</i>	<i>C-day</i>
			Annual sum of heating degree days	424–64878	<i>hdd</i>	
	Dry Bulb Temp (Hourly)	Avg. Median IQR	Annual average of dry bulb temperature	-3.11–28.39	<i>avgtdb</i>	<i>C</i>
			Median dry bulb temperature	-7.20–30	<i>medtdb</i>	
			Inter-quartile range of dry bulb Temp	3.6–34	<i>iqrtdb</i>	
	Dry Point Temp (Hourly)	Avg. Median IQR	Annual average of dry point temperature	-7.41–21.43	<i>avgtdp</i>	<i>C</i>
			Median dew point temperature	-6.4–24.2	<i>medtdp</i>	
			Inter-quartile range of dew point temperature	0–26.8	<i>iqrtdp</i>	
	Global Horizontal Irradiation (Hourly)	Avg. Sum IQR	Annual average of global horizontal irradiation	190–509	<i>avgghi</i>	<i>MWh/m2</i>
			Annual sum of global horizontal irradiation	0.40–2.23	<i>sumghi</i>	
			Inter-quartile range of global horizontal irradiation	(0.84–5.2)e-3	<i>iqrghi</i>	
	Direct Normal Irradiation (Hourly)	Avg. Sum IQR	Annual average of direct normal irradiation	57–676	<i>avgdni</i>	<i>MWh/m2</i>
			Annual sum of direct normal irradiation	-10.34–3.15	<i>sumdni</i>	
			Inter-quartile range of direct normal irradiation	(0.38–26.3)e-4	<i>iqrdni</i>	
	Humidity (Hourly)	Avg. Median	Annual average of relative humidity	22–98	<i>avrhh</i>	<i>%</i>
	Median relative humidity		18–99.6	<i>medrh</i>		

481 accuracy in term of RMSE (kWh/m^2). Rastogi et al. (2017) report an error of
482 10-15 kWh/m^2 on the EnergyPlus dataset while we achieve 6-10 kWh/m^2 . Ta-
483 bles 5 and 6 give an overview of results for the Ecotect and EnergyPlus datasets,
484 respectively. The tables contain Coefficients of Determination (R^2), Root Mean
485 Square Errors (RMSE), Mean Absolute Errors (MAE), fit time, test time, and
486 number of parameters for the best combination of hyper-parameters; the av-
487 erage fitting time of all tested models; and the total number of iterations for
488 comparison of time complexity. Here, the test time is the average of predictions
489 of all folds (192 data points per fold for Ecotect and 1,000 for Energy Plus). For
490 EnergyPlus data, GP is excluded from the comparison because the training time
491 is extremely high for large datasets. Most ML models are capable of forecasting
492 multiple outputs at the same time. However, we tuned all models separately for
493 heating and cooling loads. None of the techniques obtained the best accuracies
494 for both target values using the same combination of hyper-parameters. This
495 inconsistency indicates that the importance of input variables as well as the cor-
496 responding weights are different. Hence, two independent models are required,
497 rather than training a single model.

498 Though the datasets are drawn from different simulators, similarities in the
499 performance of the models do emerge. The lowest RMSE for both heating
500 and cooling loads is achieved by XGBoost, followed by GBRT and RF. These
501 models are all based on decision trees, but unlike RF the other two do not
502 build independent trees. Hence, they train models slightly faster than RF.
503 Considering prediction time in addition to accuracy, however, GBRT is slightly
504 faster than XGBoost but has comparable accuracy. The NN models tend to
505 have the fastest prediction times, which might make them more appropriate for
506 applications requiring very large numbers of simulation estimates. For example,
507 optimising many building parameters, each with several possible choices, under
508 a sample of uncertain operating conditions, such as the problem described in
509 (Rastogi et al., 2017). We find that GP is the slowest and least accurate model.
510 This is partially due to the challenge of using large datasets with GP regression;
511 since the time complexity of GP is $O(N^3)$ (where N is the number of data points

Table 5: Result of tuning ML model for Ecotect simulated dataset.

	SVM		RF		NN		GP		GBRT		XGBoost	
	Heat	Cool	Heat	Cool	Heat	Cool	Heat	Cool	Heat	Cool	Heat	Cool
R^2	0.996	0.972	0.998	0.973	0.997	0.968	0.981	0.944	0.999	0.995	0.999	0.998
RMSE	0.475	1.622	0.476	1.585	0.491	1.711	1.381	2.279	0.366	0.677	0.300	0.401
MAE	0.654	1.082	0.332	0.98	0.369	1.120	0.852	1.579	0.254	0.486	0.189	0.294
Fit time (s)	2.19	21.09	0.75	0.73	0.106	0.131	18.86	24.63	0.499	0.655	0.326	0.585
Mean fit time (s)	323.77	177.28	0.72	0.75	1.23	0.99	17.00	18.65	0.20	0.19	0.28	0.28
Test time	0.005	0.005	0.090	0.104	0.001	0.001	0.019	0.018	0.021	0.031	0.045	0.107
Number of parameters	2		3		7		3		7		6	
Total iteration	21		36		3240		30		3456		2160	

Table 6: Result of tuning ML model for 5000 records of EnergyPlus dataset.

	SVM		RF		NN		GBRT		XGBoost	
	Heat	Cool	Heat	Cool	Heat	Cool	Heat	Cool	Heat	Cool
R^2	0.965	0.973	0.973	0.968	0.966	0.969	0.980	0.986	0.982	0.986
RMSE	14.318	8.763	12.720	9.400	14.068	9.376	10.721	6.296	10.386	6.270
MAE	5.622	3.465	5.057	4.841	7.472	4.932	4.400	3.365	4.130	3.143
Fit time (s)	177.66	406.31	6.35	34.873	126.29	10.88	6.363	1.789	4.897	4.871
Mean fit time (s)	1641.91	1197.16	17.6	19.54	21.32	17.19	4.85	4.92	4.61	4.55
Test time	0.483	0.507	0.333	0.595	0.008	0.010	0.244	0.078	0.228	0.219
Number of parameters	2		3		7		3		7	
Total iteration	21		36		3240		3456		2160	

512 used for training/fitting), the training speed is not comparable with other ML
513 models and inversion of matrices of size $\{N, N\}$ is unfeasible for large N . Thus,
514 studies using GP have used small datasets, usually less than a few thousand
515 (Heo et al., 2012; Zhang et al., 2013; Noh & Rajagopal, 2013; Rastogi et al.,
516 2017; Burkhart et al., 2014; Zhang et al., 2015). However, since GP regression
517 allows for the automatic estimation of prediction uncertainty, it is useful in
518 some cases. An example is the estimation of summary statistics, where it is
519 more informative to know the uncertainty of, e.g., annual heating and cooling
520 loads, rather than just a point estimate. Although all models predict the energy
521 loads with high accuracy, the use case should determine the most appropriate
522 model. For example, increasing the number of records (size of training data), the
523 fitting and forecasting time of SVM rises significantly. The training size of NN
524 is slightly increased as well, but it is still the fastest predictor by a considerable
525 margin (10-20 times faster). GBRT and its variant XGBoost achieve the best
526 RMSE. However, the increased accuracy and sophistication of models like NN
527 and XGBoost comes with the penalty of requiring very large training datasets
528 (e.g., the 25,000 simulations used here). This could be an issue where a model
529 has to be trained on the fly, i.e., where simulating 25,000 distinct cases to train
530 an accurate model is prohibitively expensive. As expected, using more data to
531 fit a model increases the predictive accuracy of all models, such that complex
532 models with more parameters lose out to simpler models that have seen more
533 data, provided the simpler models can use the additional data available. In
534 summary, where sufficient training data is available and the testing or use cases
535 are not too dissimilar from the training data, the use of models such as GBRT
536 and NN improves accuracy. Where training data is harder to generate, or a
537 model must be trained on the fly with a small dataset, techniques such as GP
538 provide adequate predictions.

539 *5.1. Performance of the Best Model*

540 We now discuss the performance characteristics of the best models for each
541 dataset. The results are illustrated using two kinds of plots: predicted (esti-

542 mated) loads (\hat{y}) against loads from the simulator (y), and the distribution of
 543 errors between simulated-predicted pairs ($\hat{y} - y$). Figures 9 and 7 show the
 544 values predicted by tuned GBRT models against their corresponding simulated
 545 heating and cooling loads for the Ecotect and EnergyPlus datasets, respectively.
 546 The error distributions of these estimations are given in Figure 10 and 8.

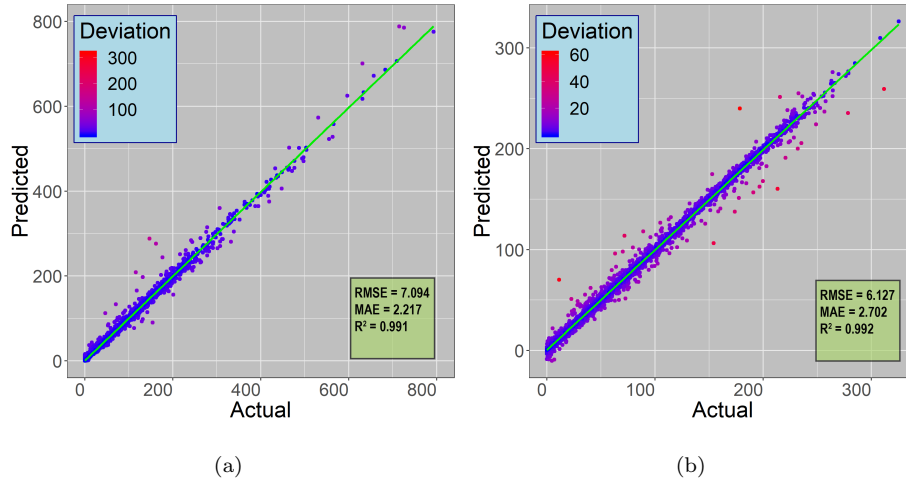
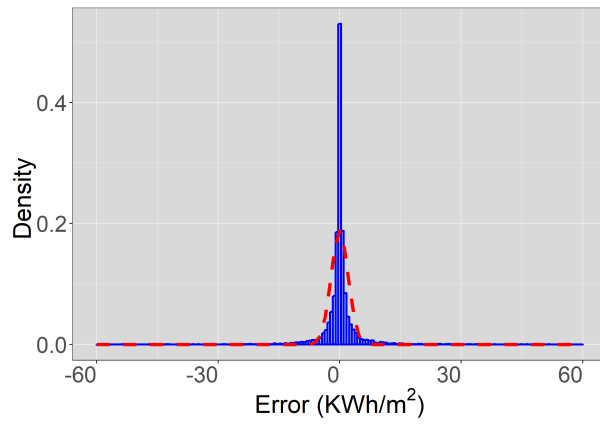


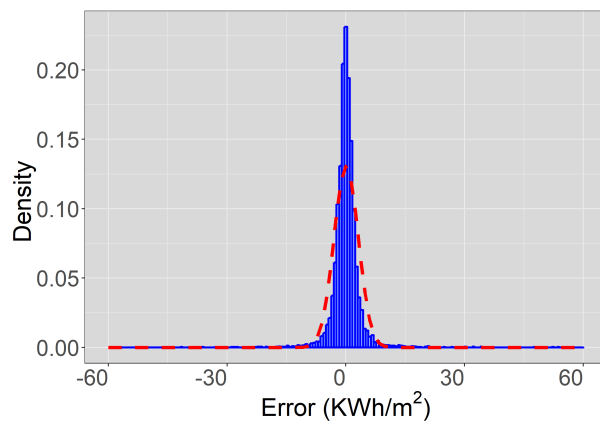
Figure 7: Actual and predicted (a) heating and (b) cooling loads of EnergyPlus dataset.

547 *5.2. Effect of Increasing Size of Training Data*

548 Given that using large datasets for training seems to improve the predictive
 549 accuracy of all models, we investigated the effect of increasing the size of the
 550 training dataset on accuracy. Figure 11 shows RMSE versus size of training
 551 dataset for the GBRT model. A 10 fold cross-validation is used to obtain the
 552 worst, best and mean RMSE over all folds. Mean training time is also displayed
 553 as the top axis to show computational cost. Although the best result is obtained
 554 by the highest number of samples tested, 25,000 is enough to build a reliable
 555 model considering the fitting time and error gap. At this point, the mean RMSE
 556 is equal to 7.770 kWh/m² and time required to fit the model is 66.02 seconds.
 557 On the other hand, using 400,000 samples and fitting over 2600 seconds, mean
 558 RMSE only goes down to 2.338 kWh/m² (4% of average heating loads).



(a)



(b)

Figure 8: Error distribution of (a) heating and (b) cooling loads prediction for EnergyPlus dataset.

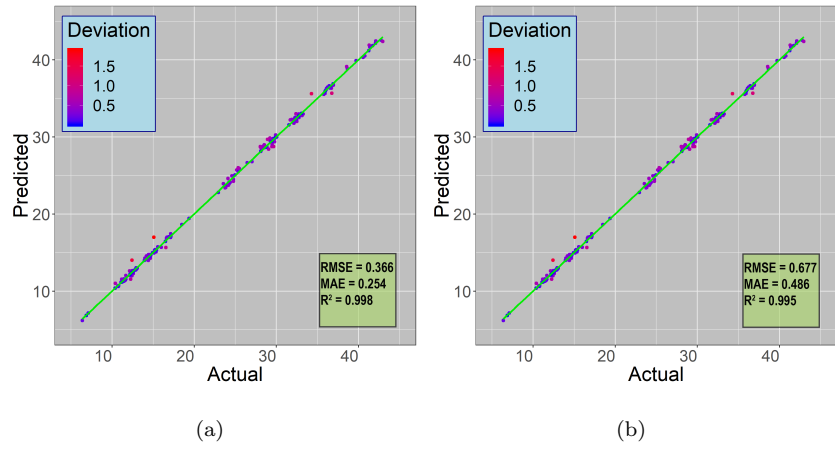


Figure 9: Actual and predicted (a) heating and (b) cooling loads of Ecotect dataset using GBRT model.

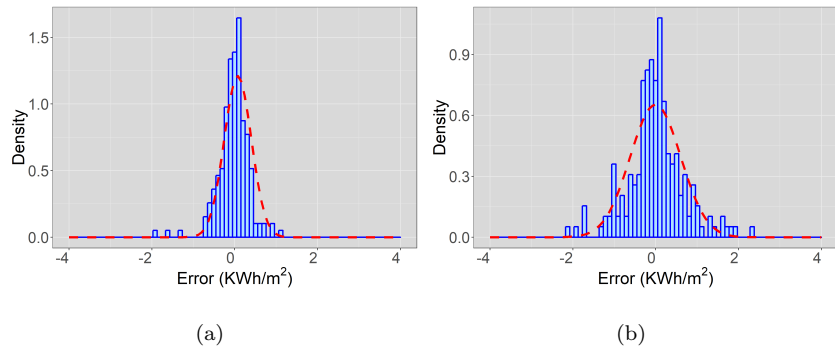


Figure 10: Error distribution of (a) heating and (b) cooling loads prediction for Ecotect dataset. The red dashed line is for a theoretical normal PDF with the same parameters.

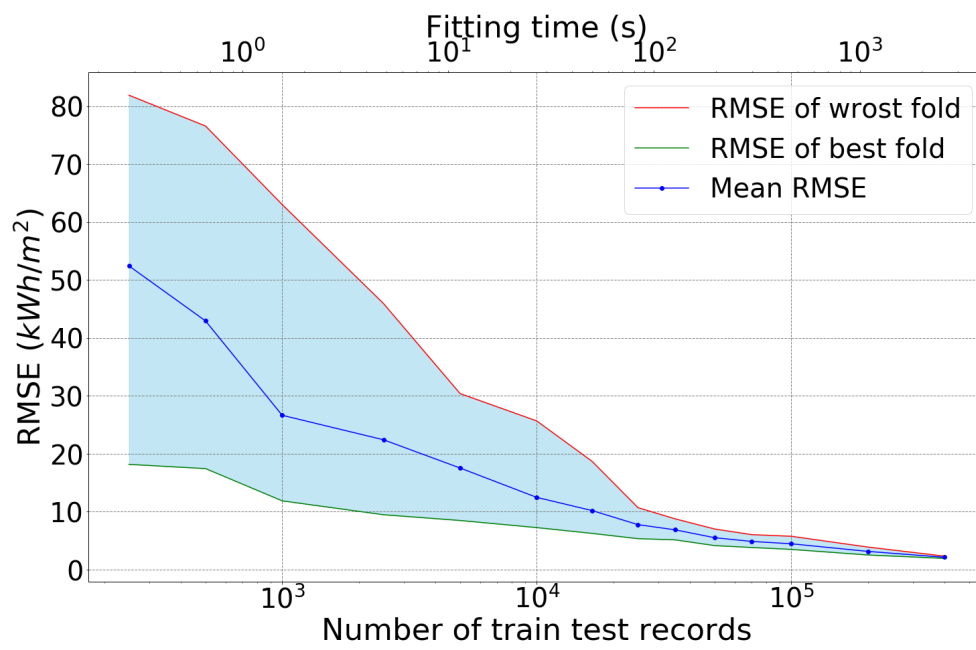


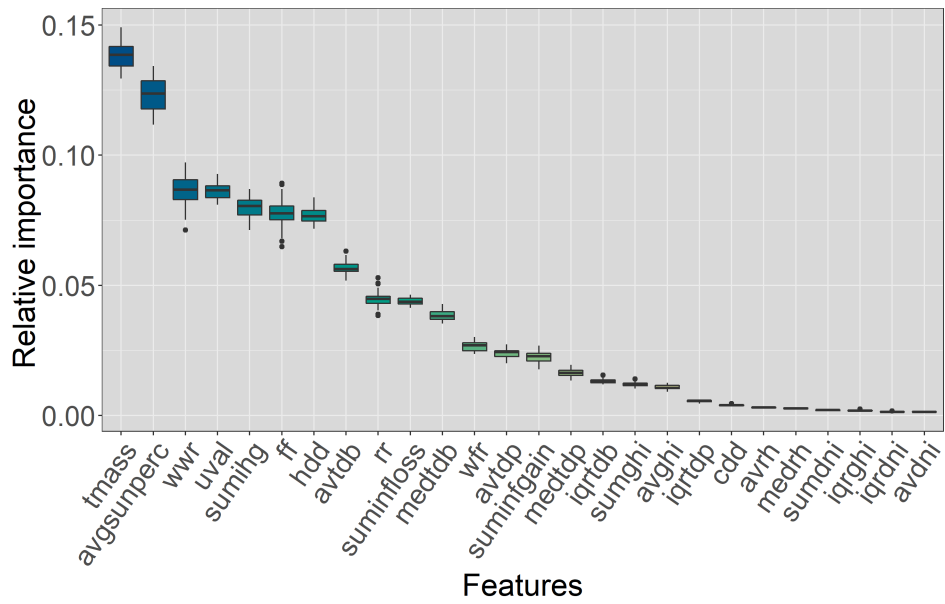
Figure 11: RMSE for heating load against number of total number of samples used for training.

559 *5.3. Feature Importance and Selection*

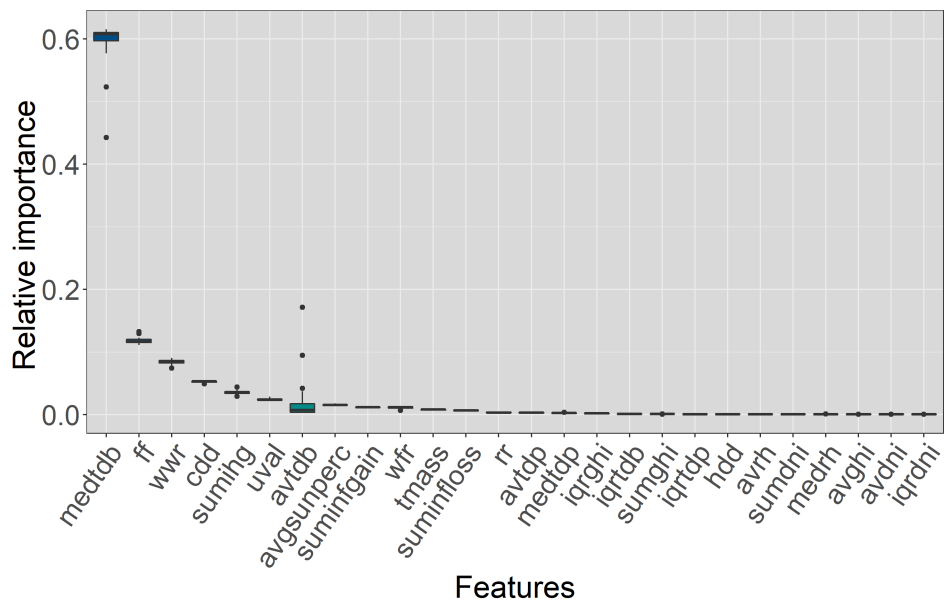
560 To emphasise the importance of features in predicting different loads, we
561 present a sensitivity analysis using two approaches. First, we present the fea-
562 ture importance calculated by the RF models. RF creates many decision trees
563 and the amount of weighted variance explained by each feature can be calcu-
564 lated for each tree. For a forest, the variance explained by each feature can be
565 averaged and the features ranked according to this measure. Here, we trained
566 30 RF models using 100,000 randomly selected samples to obtain an empirical
567 distribution of feature importance, shown in Figure 12.

568 As the best model (GBRT) doesn't provide the possibility of analysing sen-
569 sitivity to the input variables in the same way, we used a global variance-based
570 method called the Sobol method Sobol (2001); Saltelli (2002). Unlike RF, GBRT
571 does not generate unique trees. Rather, each trees is correlated to the last. To
572 facilitate a comparison, we fitted 30 different models and used them to evaluate
573 the 150,000 samples generated by the algorithm. The Sobol first-order indices
574 of features is illustrated in Figure 13. We see that the importance of features
575 to this method is less stable in GBRT than RF. However, since it is calculated
576 directly from the original data, it is more representative of the features of the
577 dataset itself.

578 For a final test, we examined the effect of dropping variables that the model
579 does not deem to be important. Based on the results of the Sobol comparison,
580 we identified the following features to drop: 'avrh', 'avdni', 'iqrdni', 'iqrghi',
581 'medrh', 'sumdni' for both loads, and 'avghi', 'sumghi' for cooling only. All
582 of the dropped variables are climate-related, which implies that there may be
583 too many variables used to explain variance due to climate. The GBRT with
584 fewer features was also trained and tested over 10 folds with 25,000 random
585 samples. The results of training a model with a reduced feature set is compared
586 with using the full set of features in Table 7. We see that removing features to
587 which the model is apparently insensitive does not negatively affect the model
588 performance. However, the time complexity of training model is reduced due to
589 a reduction in the size of the dataset. Given that this result applies only to this

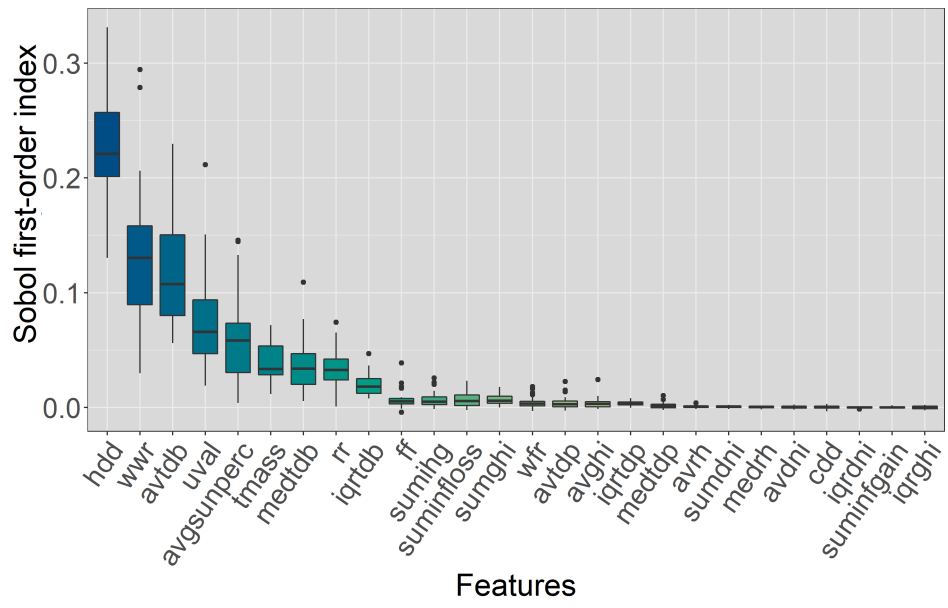


(a)

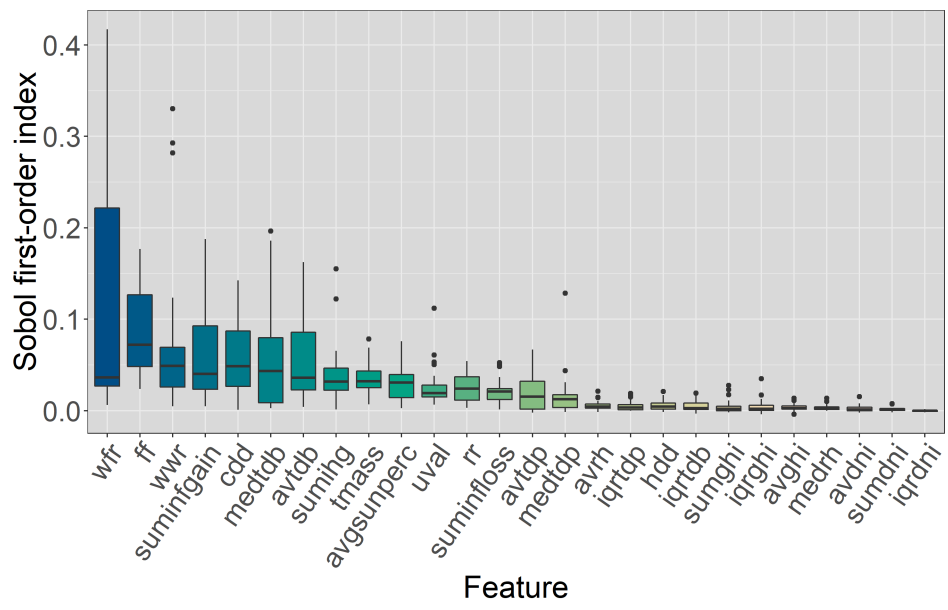


(b)

Figure 12: Importance of features for (a) heating and (b) cooling loads prediction using RF model.



(a)



(b)

Figure 13: Sobol first-order indices of features in predicting (a) heating and (b) cooling loads using best ML model.

590 dataset and cannot be generalised to all buildings or EnergyPlus simulations,
 591 this is not a repeatable result unless we are confident that the dataset used for
 592 training represents the use case or problem completely.

Table 7: Performance comparison of ML models with full and reduced feature sets determined by sensitivity analysis.

	Heating Load		Cooling Load	
	All inputs	Selected inputs	All inputs	Selected inputs
RMSE	7.871	7.648	4.455	4.384
MAE	2.127	2.085	2.314	2.310
R^2	0.991	0.991	0.993	9.993
Fit time (s)	61.621	48.420	9.387	7.700
Test time (s)	0.642	0.622	0.151	0.145

593 6. Conclusion

594 The research presented in this paper addresses the gap in using ML methods
 595 for estimating building energy loads through a comprehensive study of common
 596 ML models fitting over energy simulation data. As became evident in the re-
 597 viewed literature, despite the wide usage of MLs in this field, a conclusion on
 598 selecting the right model for the energy prediction was not possible. The main
 599 reason is that most of the research works have focused on the first eminent
 600 part of statistical modelling which is features selection. This paper discussed
 601 the importance of ML model optimisation in providing a fair comparison of dif-
 602 ferent methods in term of accuracy, the simplicity of tuning and training and
 603 response times of model. This study optimised the hyper-parameters of each
 604 model for both heating and cooling loads to obtain the best precision. It was
 605 also indicated that when there are two energy indices as cooling and heating
 606 loads to be estimated by model, it is desired to optimise and train separate

607 machines. To that end, the role of ML model in recognising most impacting
608 factor in prediction of building loads. The other key outcome of this research
609 is a set of recommendations for the quick selection of ML model based on the
610 data and usage.

611 The results indicated that the standard and advanced GBRTs provide the
612 most accurate predictions, considering the RMSE value. However, when the
613 data was simple (in term of input variables and size), SVM was proven to be the
614 best choice because of simplicity and the speed of calculations. The results also
615 ascertained that for complex data sets, multi-layer NNs are more appropriate
616 when there is a massive demand for ever-more energy simulations. In this case,
617 NN was proven to be capable of estimating incredibly faster than other MLs
618 methods. It should be noted that NN is complicated, and requires an expert to
619 particularly tune it for each studied case; otherwise, NNs could fail quickly.

620 Comparison of tuned models with previous studies highlighted the impor-
621 tance of determining the hyper-parameters for each data set, and the fact that
622 this can become more crucial by increasing the size and intricacy of the ex-
623 aminations set. By fitting individual models for heating and cooling loads, it
624 was shown that one assorted set of model parameters could not accurately esti-
625 mate both values. Therefore, unlike previous studies, it is recommended by this
626 study to train models for each energy load independently. The other approach
627 would be the implementation of a specific sorting algorithm to find balanced
628 values. As results signified, it is suggested to attain a higher accuracy feeding
629 the machines with more number of instances is essential. It might not be a
630 solution for measured historical data; however further simulation using various
631 values of inputs could be aggregated during the design stage prior to optimising
632 the building. Another identified critical factor was that the features must be
633 thoroughly selected/created for representing building characteristics and needs
634 should be appropriately investigated before developing models.

635 The findings of this study concurred with the seminal literature by demon-
636 strating the fact that MLs techniques are overtly superior over the conventional
637 statistical and engineering methods in building energy calculation. This study

638 also revealed the further power of those ML methods and newly developed ones
639 when they thoroughly optimised. There are several ready to use software pack-
640 ages (e.g. Matlab) providing various ML models with few parameters to modify.
641 Nevertheless, it is advisable to use simpler models like SVM or RF with an ad-
642 vanced programming language, such as Python and R.

643 Finally, the most important features are recognised using sensitivity analysis
644 methods, and the investigation of the model with reduced dimension revealed
645 that even though the computational cost of building model is reduced, the
646 performance didn't alter. This analysis demonstrated the capability of MLs
647 in eliminating inessential input parameters, while most statistical methods are
648 susceptible to these type of features.

649 The methods discussed in this work proved the efficiency of ML models in
650 predicting building energy loads as well as performance. The fast and accurate
651 calculation of those values paves pathways for more informed and productive de-
652 sign decisions for built environments. Furthermore, along with the optimisation
653 algorithms, ML seems as a promising solution for efficacious retrofit planning of
654 complex buildings, where engineers are not capable of massive calculations.

655 **Appendix A. Detailed Results for Tuning ML Models**

656 The detail of tuning each ML model is presented in this section. Some
657 models have several parameters, so the brute force search includes thousands of
658 train-test models. Therefore, it is not possible to present the list of all results
659 in this paper. However, Tables A.8 to A.13 demonstrates the parameters for the
660 best models predicting energy loads of both datasets. In each table the best
661 model is highlighted with light blue colour.

662 In order to reduce the time complexity of tuning ANN model, the number
663 of epochs was fixed at 500 and the other parameters were optimised. Then
664 the optimal number of propagations was separately obtained using the best
665 parameters. As shown in the Figures A.14 (a) and (b)

Table A.8: Detail of optimising SVM for both datasets.

EPlus Data		Ecotect Data		SVM Parameters	
Heat RMSE	Cool RMSE	Heat RMSE	Cool RMSE	C	Gamma
14.318	9.785	0.677	1.622	10,000	1
18.988	9.774	0.654	1.667	1000	1
15.720	9.261	0.660	1.756	1,000,000	0.1
15.313	10.302	0.978	1.842	1,000,000	1
21.626	8.763	0.815	2.048	100,000	0.1
31.415	9.452	2.108	2.636	10,000	0.1
43.719	17.833	2.627	3.365	10,000	0.01
60.974	31.658	3.304	3.886	1	0.1
60.974	31.658	3.304	6.550	1	0.01

Table A.9: Detail of optimising RF for both datasets.

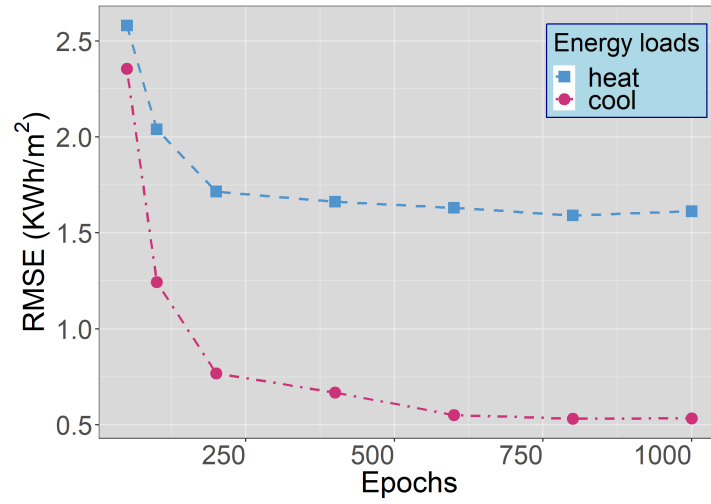
EPlus Data		Ecotect Data		RF Parameters		
Heat RMSE	Cool RMSE	Heat RMSE	Cool RMSE	Bootstrap	Max features	No. of estimators
12.873	9.894	0.568	1.585	False	sqrt	600
12.720	9.693	0.576	1.605	False	sqrt	400
14.556	10.734	0.604	1.612	True	sqrt	200
13.334	10.214	0.502	1.658	False	log2	1000
14.551	9.691	0.476	1.683	True	auto	600
14.584	9.600	0.478	1.691	True	auto	800
24.189	13.727	0.536	1.814	False	auto	1000
14.199	10.995	0.616	1.604	True	sqrt	400

Table A.10: Detail of optimising GBRT for both datasets.

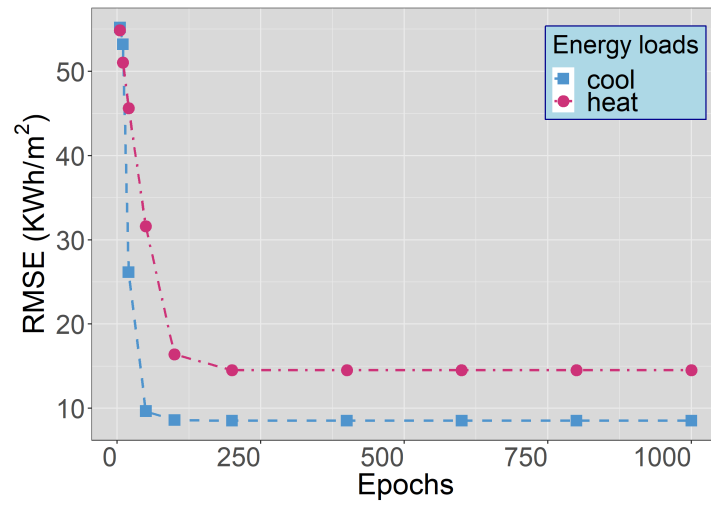
EPlus Data			Ecotect Data			GBRT Parameters					
Heat RMSE	Cool RMSE	Heat RMSE	Cool RMSE	Learning rate	Max depth	max features	Min sample leaf	Min sample split	No. estimator	Sub sample	
13.157	7.402	0.388	0.677	0.15	8	None	1	100	1500	1	
11.534	6.667	0.366	0.893	0.15	3	None	1	2	1500	1	
12.914	6.297	0.399	1.033	0.25	3	sqrt	1	2	1500	1	
10.721	8.855	0.514	1.261	0.1	8	sqrt	1	2	2000	1	
13.257	9.608	0.523	1.578	0.01	13	sqrt	1	2	1250	0.9	
17.843	8.654	3.77	3.895	0.01	8	sqrt	200	100	500	1	
22.775	9.856	8.732	8.524	0.001	13	sqrt	200	100	1250	0.7	
26.221	15.625	10.054	9.725	0.25	3	sqrt	1000	100	1750	1	
35.518	21.196	10.003	9.726	0.1	8	sqrt	1000	1000	1000	0.9	
46.991	24.279	9.996	9.720	0.1	3	sqrt	1000	2	1000	0.8	
49.515	24.542	9.996	9.722	0.1	3	None	1000	100	1500	0.7	
21.578	11.642	10.422	9.746	0.15	13	None	500	1000	1000	0.8	

Table A.11: Detail of optimising XGBoost for both datasets.

EPlus Data			Ecotect Data			XGBoost Parameters				
Heat RMSE	Cool RMSE	Heat RMSE	Cool RMSE	Portion of features	Learning rate	Max depth	Min child weight	No. estimator	Sub sample	
10.909	8.145	0.303	0.401	0.6	0.1	8	1	1750	0.9	
11.616	9.002	0.300	0.452	0.6	0.1	13	1	750	0.7	
12.273	8.048	0.323	0.573	0.38	0.1	8	1	1250	0.8	
12.436	8.18	0.329	0.804	0.6	0.01	13	1	1750	1	
11.302	6.270	0.413	1.131	0.6	0.1	3	1	2000	0.7	
10.387	6.382	0.409	1.115	0.6	0.1	3	3	2000	0.9	
13.738	9.982	0.306	0.443	0.5	0.1	13	1	1750	0.8	
16.030	12.706	0.337	0.557	0.4	0.5	13	3	1000	0.7	
20.003	10.434	0.304	0.433	0.1	0.1	8	1	10000	0.8	
23.821	14.138	0.343	0.567	0.1	0.25	13	3	1000	0.7	
26.266	16.581	0.365	0.578	0.1	0.5	13	3	1500	0.8	
57.263	35.554	9.459	10.412	0.6	0.01	3	1	200	0.7	



(a)



(b)

Figure A.14: RMSE of ANN model predicting energy loads for (a) EPlus and (b) Ecotects datasets against number of epochs.

Table A.12: Detail of optimising GP for both datasets.

Ecotect Data		GP Parameters		
Heat RMSE	Cool RMSE	Alpha	Kernel	No. restarts
1.382	2.279	1e-08	Mattern	2
1.381	2.383	1e-12	RBF	4
8.472	2.332	1e-8	RBF	2
8.471	2.333	1e-10	RBF	0
1.383	3.138	1e-4	Mattern	0
4.440	4.238	1e-6	RBF	4

References

- Ascione, F., Bianco, N., De Stasio, C., Mauro, G. M., & Vanoli, G. P. (2017). Artificial neural networks to predict energy performance and retrofit scenarios for any member of a building category: A novel approach. *Energy*, *118*, 999–1017. URL: <http://dx.doi.org/10.1016/j.energy.2016.10.126>. doi:10.1016/j.energy.2016.10.126.
- Breiman, L. (2017). *Classification and regression trees*. Routledge.
- Bukkapatnam, S. T., & Cheng, C. (2010). Forecasting the evolution of nonlinear and nonstationary systems using recurrence-based local Gaussian process models. *Physical Review E - Statistical, Nonlinear, and Soft Matter Physics*, *82*, 56206. doi:<https://doi.org/10.1103/PhysRevE.82.056206>.
- Burkhart, M. C., Heo, Y., & Zavala, V. M. (2014). Measurement and verification of building systems under uncertain data: A Gaussian process modeling approach. *Energy and Buildings*, *75*, 189–198. URL: <http://dx.doi.org/10.1016/j.enbuild.2014.01.048>. doi:10.1016/j.enbuild.2014.01.048.
- Chen, T., & Guestrin, C. (2016). XGBoost: A Scalable Tree Boosting System. In *Proceedings of the 22nd acm sigkdd international conference on knowledge*

Table A.13: Detail of optimising ANN for both datasets.

EPlus Data		Ecotect Data		ANN Parameters				
Heat RMSE	Cool RMSE	Heat RMSE	Cool RMSE	Activation	Batch size	No. hidden layers	No. neurons	Optimiser
30.456	12.103	0.492	1.829	Logistic	10	1	2N	lbfgs
30.675	15.847	0.781	1.711	Tanh	10	1	2N	lbfgs
14.631	9.973	0.884	3.389	Tanh	1	2	N, 2N	adam
17.337	9.376	1.052	3.308	Tanh	10	3	3N, 2N, N	lbfgs
14.068	9.754	2.616	3.388	Tanh	1	1	2N	adam
41.157	18.079	4.476	6.645	Relu	1	2	N, 2N	adam
27.573	13.994	10.005	9.73	Logistic	10	3	3N, 2N, N	adam
51.323	26.502	14.453	15.968	Relu	auto	1	N	adam
49.118	25.223	6.401	7.010	Identity	1	2	N, N/2	adam
80.052	57.114	23.506	25.482	Logistic	10	2	3N, N/2	adam

- discovery and data mining* (pp. 785–794). ACM. doi:<https://doi.org/10.1145/2939672.2939785>.
- Chen, Y., & Tan, H. (2017). Short-term prediction of electric demand in building sector via hybrid support vector regression. *Applied Energy*, *204*, 1363–1374. doi:<https://doi.org/10.1016/j.apenergy.2017.03.070>.
- Chinazzo, G., Rastogi, P., & Andersen, M. (2015). Assessing robustness regarding weather uncertainties for energy-efficiency-driven building refurbishments. *Energy Procedia*, *78*, 931–936.
- Deb, C., Eang, L. S., Yang, J., & Santamouris, M. (2016). Forecasting diurnal cooling energy load for institutional buildings using Artificial Neural Networks. *Energy and Buildings*, *121*, 284–297. URL: <http://dx.doi.org/10.1016/j.enbuild.2015.12.050>. doi:10.1016/j.enbuild.2015.12.050.
- DOE (). Commercial Reference Buildings. URL: <https://www.energy.gov/eere/buildings/commercial-reference-buildings>.
- Dombayci, Ö. A. (2010). The prediction of heating energy consumption in a model house by using artificial neural networks in Denizli-Turkey. *Advances in Engineering Software*, *41*, 141–147. doi:<https://doi.org/10.1016/j.advengsoft.2009.09.012>.
- Dong, B., Cao, C., & Lee, S. E. (2005). Applying support vector machines to predict building energy consumption in tropical region. *Energy and Buildings*, *37*, 545–553. doi:10.1016/j.enbuild.2004.09.009.
- Edwards, R. E., New, J., & Parker, L. E. (2012). Predicting future hourly residential electrical consumption: A machine learning case study. *Energy and Buildings*, *49*, 591–603. URL: <http://dx.doi.org/10.1016/j.enbuild.2012.03.010>. doi:10.1016/j.enbuild.2012.03.010.
- Ghiassi, M., Saidane, H., & Zimbra, D. (2005). A dynamic artificial neural network model for forecasting time series events. *International Journal of Fore-*

- casting*, 21, 341–362. doi:<https://doi.org/10.1016/j.ijforecast.2004.10.008>.
- Grosicki, E., Abed-Meraim, K., & Hua, Y. (2005). A weighted linear prediction method for near-field source localization. *IEEE Transactions on Signal Processing*, 53, 3651–3660. doi:<https://doi.org/10.1109/TSP.2005.855100>.
- Harpham, C., & Dawson, C. W. (2006). The effect of different basis functions on a radial basis function network for time series prediction: a comparative study. *Neurocomputing*, 69, 2161–2170. doi:<https://doi.org/10.1016/j.neucom.2005.07.010>.
- Heo, Y., Choudhary, R., & Augenbroe, G. A. (2012). Calibration of building energy models for retrofit analysis under uncertainty. *Energy and Buildings*, 47, 550–560. URL: <http://dx.doi.org/10.1016/j.enbuild.2011.12.029>. doi:10.1016/j.enbuild.2011.12.029.
- Heo, Y., & Zavala, V. M. (2012). Gaussian process modeling for measurement and verification of building energy savings. *Energy and Buildings*, 53, 7–18. URL: <http://dx.doi.org/10.1016/j.enbuild.2012.06.024>. doi:10.1016/j.enbuild.2012.06.024.
- Hong, S. M., Paterson, G., Burman, E., Steadman, P., & Mumovic, D. (2014a). A comparative study of benchmarking approaches for non-domestic buildings: Part 1 Top-down approach. *International Journal of Sustainable Built Environment*, 2, 119–130. URL: <http://dx.doi.org/10.1016/j.ijjsbe.2014.04.001>. doi:10.1016/j.ijjsbe.2014.12.001.
- Hong, S.-M., Paterson, G., Mumovic, D., & Steadman, P. (2014b). Improved benchmarking comparability for energy consumption in schools. *Building Research & Information*, 42, 47–61. URL: <http://www.tandfonline.com/doi/abs/10.1080/09613218.2013.814746>. doi:10.1080/09613218.2013.814746.

- Hou, Z., & Lian, Z. (2009). An application of support vector machines in cooling load prediction. In *Intelligent Systems and Applications, 2009. ISA 2009. International Workshop on* (pp. 1–4). IEEE.
- Jain, R. K., Smith, K. M., Culligan, P. J., & Taylor, J. E. (2014). Forecasting energy consumption of multi-family residential buildings using support vector regression: Investigating the impact of temporal and spatial monitoring granularity on performance accuracy. *Applied Energy*, *123*, 168–178. URL: <http://dx.doi.org/10.1016/j.apenergy.2014.02.057>. doi:10.1016/j.apenergy.2014.02.057.
- Kalogirou, S., Florides, G., Neocleous, C., & Schizas, C. (2001). Estimation of Daily Heating and Cooling Loads Using Artificial Neural Networks. In *Proceedings of CLIMA 2000 International Conference* September (pp. 15–18). Naples.
- Kalogirou, S., Neocleous, C., & Schizas, C. (1997). Building Heating Load Estimation Using Artificial Neural Networks. In *Proceedings of the 17th international conference on Parallel architectures and compilation techniques* (pp. 1–8). volume 8. URL: http://www.inive.org/members/{_}area/medias/pdf/Inive/clima2000/1997/P159.pdf.
- Khayatian, F., Sarto, L., & Dall’O’, G. (2016). Application of neural networks for evaluating energy performance certificates of residential buildings. *Energy and Buildings*, *125*, 45–54. URL: <http://dx.doi.org/10.1016/j.enbuild.2016.04.067>. doi:10.1016/j.enbuild.2016.04.067.
- Leung, H., Lo, T., Member, S., & Wang, S. (2001). Prediction of Noisy Chaotic Time Series Using an Optimal Radial Basis Function Neural Network. *IEEE Transactions on Neural Networks*, *12*, 1163–1172. doi:<https://doi.org/10.1109/72.950144>.
- Li, K., Hu, C., Liu, G., & Xue, W. (2015). Building’s electricity consumption prediction using optimized artificial neural networks and principal component

- analysis. *Energy and Buildings*, 108, 106–113. URL: <http://dx.doi.org/10.1016/j.enbuild.2015.09.002>. doi:10.1016/j.enbuild.2015.09.002.
- Li, Q., Meng, Q., Cai, J., Yoshino, H., & Mochida, A. (2009). Predicting hourly cooling load in the building: A comparison of support vector machine and different artificial neural networks. *Energy Conversion and Management*, 50, 90–96. URL: <http://dx.doi.org/10.1016/j.enconman.2008.08.033>. doi:10.1016/j.enconman.2008.08.033.
- Li, Q., Ren, P., & Meng, Q. (2010). Prediction model of annual energy consumption of residential buildings. In *Advances in Energy Engineering (ICAEE), 2010 International Conference on* (pp. 223–226). IEEE.
- Li, Z., Han, Y., & Xu, P. (2014). Methods for benchmarking building energy consumption against its past or intended performance: An overview. URL: <http://www.sciencedirect.com/science/article/pii/S0306261914002505>. doi:10.1016/j.apenergy.2014.03.020.
- Massana, J., Pous, C., Burgas, L., Melendez, J., & Colomer, J. (2015). Short-term load forecasting in a non-residential building contrasting models and attributes. *Energy and Buildings*, 92, 322–330. doi:10.1016/j.enbuild.2015.02.007.
- Mena, R., Rodríguez, F., Castilla, M., & Arahál, M. R. (2014). A prediction model based on neural networks for the energy consumption of a bioclimatic building. *Energy and Buildings*, 82, 142–155. URL: <http://dx.doi.org/10.1016/j.enbuild.2014.06.052>. doi:10.1016/j.enbuild.2014.06.052.
- Neto, A. H., & Fiorelli, F. A. S. (2008). Comparison between detailed model simulation and artificial neural network for forecasting building energy consumption. *Energy and Buildings*, 40, 2169–2176. doi:10.1016/j.enbuild.2008.06.013.
- Noh, H. Y., & Rajagopal, R. (2013). Data-driven forecasting algorithms for building energy consumption. In *Sensors and Smart Structures Technologies*

- for *Civil, Mechanical, and Aerospace Systems* (p. 86920T). San Diego: SPIE volume 8692. URL: <http://www.scopus.com/inward/record.url?eid=2-s2.0-84878736246&partnerID=tZ0tx3y1>. doi:10.1117/12.2009894.
- Owen, D. B., Abramowitz, M., & Stegun, I. A. (1965). *Handbook of Mathematical Functions with Formulas, Graphs, and Mathematical Tables* volume 7. Courier Corporation. doi:<https://doi.org/10.2307/1266136>. arXiv:1701.01870.
- Papadopoulos, S., Azar, E., Woon, W.-L., & Kontokosta, C. E. (2017). Evaluation of tree-based ensemble learning algorithms for building energy performance estimation. *Journal of Building Performance Simulation*, 1493, 1–11. doi:<https://doi.org/10.1080/19401493.2017.1354919>.
- Park, B., Messer, C. J., & Urbanik II, T. (1998). Short-term freeway traffic volume forecasting using radial basis function neural network. *Transportation Research Record: Journal of the Transportation Research Board*, 1651, 39–47. doi:<https://doi.org/10.3141/1651-06>.
- Park, Y.-S., & Lek, S. (2016). Artificial Neural Networks: Multilayer Perceptron for Ecological Modeling. In *Developments in Environmental Modelling* (pp. 123–140). Wiley Online Library. doi:<https://doi.org/10.1016/B978-0-444-63623-2.00007-4>.
- Paudel, S., Elmtiri, M., Kling, W. L., Corre, O. L., & Lacarrière, B. (2014). Pseudo dynamic transitional modeling of building heating energy demand using artificial neural network. *Energy and Buildings*, 70, 81–93. URL: <http://dx.doi.org/10.1016/j.enbuild.2013.11.051>. doi:10.1016/j.enbuild.2013.11.051.
- Platon, R., Dehkordi, V. R., & Martel, J. (2015). Hourly prediction of a building's electricity consumption using case-based reasoning, artificial neural networks and principal component analysis. *Energy and Buildings*, 92, 10–18. URL: <http://dx.doi.org/10.1016/j.enbuild.2015.01.047>. doi:10.1016/j.enbuild.2015.01.047.

- Rastogi, P. (2016). *On the sensitivity of buildings to climate: the interaction of weather and building envelopes in determining future building energy consumption*. Ph.D. thesis Ecole Polytechnique Fédérale de Lausanne. URL: https://infoscience.epfl.ch/record/220971/files/EPFL_{_}TH6881.pdf.
- Rastogi, P., & Andersen, M. (2016). Incorporating Climate Change Predictions in the Analysis of Weather-Based Uncertainty. *Proceedings of SimBuild*, 6.
- Rastogi, P., Polytechnique, E., & Lausanne, F. D. (2017). Gaussian-Process-Based Emulators for Building Performance Simulation. In *Building Simulation 2017: The 15th International Conference of IBPSA*. San Francisco: IBPSA.
- Saltelli, A. (2002). Sensitivity analysis for importance assessment. *Risk analysis*, 22, 579–590.
- Seyedzadeh, S., Rahimian, F. P., Glesk, I., & Roper, M. (2018). Machine learning for estimation of building energy consumption and performance: a review. *Visualization in Engineering*, 6, 5. doi:<https://doi.org/10.1186/s40327-018-0064-7>.
- Si, J. (2017). *Green retrofit of existing non-domestic buildings as a multi criteria decision making process by*. Ph.D. thesis.
- Sobol, I. M. (2001). Global sensitivity indices for nonlinear mathematical models and their Monte Carlo estimates. *Mathematics and computers in simulation*, 55, 271–280.
- Tin Kam Ho (1995). Random decision forests. In *Proceedings of 3rd International Conference on Document Analysis and Recognition* (pp. 278–282). IEEE volume 1. doi:<https://doi.org/10.1109/ICDAR.1995.598994>.
- Tsanas, A., & Xifara, A. (2012). Accurate quantitative estimation of energy performance of residential buildings using statistical machine learning tools. *Energy and Buildings*, 49, 560–567. doi:10.1016/j.enbuild.2012.03.003.

- Tso, G. K. F., & Yau, K. K. W. (2007). Predicting electricity energy consumption : A comparison of regression analysis , decision tree and neural networks. *Energy*, *32*, 1761–1768. doi:<https://doi.org/10.1016/j.energy.2006.11.010>.
- Wang, Z., Wang, Y., Zeng, R., Srinivasan, R. S., & Ahrentzen, S. (2018). Random Forest based hourly building energy prediction. *Energy and Buildings*, *171*, 11–25. doi:<https://doi.org/10.1016/j.enbuild.2018.04.008>.
- Wong, S. L., Wan, K. K. W., & Lam, T. N. T. (2010). Artificial neural networks for energy analysis of office buildings with daylighting. *Applied Energy*, *87*, 551–557. URL: <http://linkinghub.elsevier.com/retrieve/pii/S0306261909002669>. doi:10.1016/j.apenergy.2009.06.028.
- Xifara, A., & Tsanas, A. (2012). Energy efficiency Data Set.
- Xuemei, L. X. L., Jin-hu, L. J.-h. L., Lixing, D. L. D., Gang, X. G. X., & Jibin, L. J. L. (2009). Building Cooling Load Forecasting Model Based on LS-SVM. *Asia-Pacific Conference on Information Processing*, *1*, 55–58. doi:10.1109/APCIP.2009.22.
- Yalcintas, M. (2006). An energy benchmarking model based on artificial neural network method with a case example for tropical climates. *International Journal of Energy Research*, *30*, 1158–1174. doi:10.1002/er.1212.
- Yalcintas, M., & Ozturk, U. A. (2007). An energy benchmarking model based on artificial neural network method utilizing US Commercial Buildings Energy Consumption Survey (CBECS) database. *International Journal of Energy Research*, *31*, 412–421. doi:10.1002/er.1232. arXiv:arXiv:1011.1669v3.
- Yokoyama, R., Wakui, T., & Satake, R. (2009). Prediction of energy demands using neural network with model identification by global optimization. *Energy Conversion and Management*, *50*, 319–327. URL: <http://dx.doi.org/10.1016/j.enconman.2008.09.017>. doi:10.1016/j.enconman.2008.09.017.

- Zhang, Y., O'Neill, Z., Dong, B., & Augenbroe, G. (2015). Comparisons of inverse modeling approaches for predicting building energy performance. *Building and Environment*, *86*, 177–190. URL: <http://dx.doi.org/10.1016/j.buildenv.2014.12.023>. doi:10.1016/j.buildenv.2014.12.023.
- Zhang, Y., O'Neill, Z., Wagner, T., & Augenbroe, G. (2013). An inverse model with uncertainty quantification to estimate the energy performance of an office building. *IBPSA Building Simulation*, (pp. 614–621). URL: <http://www.ibpsa.org/proceedings/BS2013/p{ }1410.pdf>.
- Zhao, H.-x., & Magoulès, F. (2010). Parallel Support Vector Machines Applied to the Prediction of Multiple Buildings Energy Consumption. *Journal of Algorithms & Computational Technology*, *4*, 231–249. doi:10.1260/1748-3018.4.2.231.
- Zhao, H. X., & Magoulès, F. (2012a). A review on the prediction of building energy consumption. *Renewable and Sustainable Energy Reviews*, *16*, 3586–3592. doi:10.1016/j.rser.2012.02.049.
- Zhao, H.-X., & Magoulès, F. (2012b). Feature Selection for Predicting Building Energy Consumption Based on Statistical Learning Method. *Journal of Algorithms & Computational Technology*, *6*, 59–77. URL: <http://journals.sagepub.com/doi/10.1260/1748-3018.6.1.59>. doi:10.1260/1748-3018.6.1.59.